

The worst approximable rational numbers

Boris Springborn

Abstract

We classify and enumerate all rational numbers with approximation constant at least $\frac{1}{3}$ using hyperbolic geometry. Rational numbers correspond to geodesics in the modular torus with both ends in the cusp, and the approximation constant measures how far they stay out of the cusp neighborhood in between. Compared to the original approach, the geometric point of view eliminates the need to discuss the intricate symbolic dynamics of continued fraction representations, and it clarifies the distinction between the two types of worst approximable rationals: (1) There is a plane forest of *Markov fractions* whose denominators are Markov numbers. They correspond to simple geodesics in the modular torus with both ends in the cusp. (2) For each Markov fraction, there are two infinite sequences of *companions*, which correspond to non-simple geodesics with both ends in the cusp that do not intersect a pair of disjoint simple geodesics, one with both ends in the cusp and one closed.

MSC (2010). 10F20, 30F60

Key words and phrases. Approximation constant, Diophantine approximation, Markov equation, modular torus

1 Introduction

For any real number x , the *approximation constant*

$$C(x) = \inf_{\frac{p}{q} \in \mathbb{Q} \setminus \{x\}} q^2 \cdot \left| x - \frac{p}{q} \right|, \quad (1)$$

measures how well x can be approximated by rational numbers $\frac{p}{q} \neq x$. Excluding x from the admissible approximants $\frac{p}{q}$ makes $C(x)$ strictly positive for all rational numbers x . (This is easy to see and will be discussed shortly.) Intuitively, the larger the approximation constant $C(x)$ of a rational number $x \in \mathbb{Q}$, the more isolated the rational number x is among the other rational numbers.

An *irrational* number x is sometimes called *badly approximable* if $C(x) > 0$, and this is the case if and only if the sequence of partial denominators a_k of the continued fraction expansion

$$x = a_0 + \frac{1}{a_1 + \frac{1}{a_2 + \dots}}$$

is bounded (see, e.g., [1, Prop. 1.32] or [19, §10.8]).

By contrast (as stated before) $C(x) > 0$ for all rational numbers $x = \frac{p_0}{q_0}$. Moreover, the nonzero infimum in (1) is attained for some fraction $\frac{p}{q}$ with smaller denominator, $q \leq q_0$. Because, on the one hand, if $q > q_0$ and $\frac{p}{q} \neq \frac{p_0}{q_0}$, then

$$q^2 \cdot \left| \frac{p_0}{q_0} - \frac{p}{q} \right| = \frac{q}{q_0} \cdot |p_0q - q_0p| > 1.$$

On the other hand, if $q = 1$ and p is a closest integer to x (except x itself if $x \in \mathbb{Z}$) then

$$q^2 \cdot \left| x - \frac{p}{q} \right| = |x - p| \leq 1$$

with equality if and only if $x \in \mathbb{Z}$.

This shows not only that all rational numbers are badly approximable in the sense that $C(x) > 0$, but also that the very worst approximable rational numbers are the integers $x \in \mathbb{Z}$ with $C(x) = 1$. They are followed by the half-integers $x \in \mathbb{Z} + \frac{1}{2}$ with $C(x) = \frac{1}{2}$, which are best approximated by the two the nearest integers. This can be seen as a striking confirmation of Hardy and Wright's general observation: "From the point of view of rational approximation, *the simplest numbers are the worst*" [19, p. 209, emphasis in original].

This article is about a geometric method to classify and enumerate the rational numbers x with approximation constant $C(x) \geq \frac{1}{3}$. Previously, the real numbers with $C(x) > \frac{1}{3}$ were classified in terms of their continued fraction representations by Flahive [14] for rational x and by Gurwood [17] for irrational x . Flahive's classification apparently extends to include rational numbers with $C(x) = \frac{1}{3}$.

All of this is closely related to the classification of *Markov irrationals* and *Markov forms*, i.e., of irrational numbers x with *Lagrange number* $L(x) > \frac{1}{3}$ and of indefinite quadratic forms $f(x, y) = ax^2 + 2bxy + cy^2$ with *Markov constant* $M(f) > \frac{2}{3}$, where

$$L(x) = \liminf_{q \rightarrow \infty} \left(q^2 \cdot \min_{p \in \mathbb{Z}} \left| x - \frac{p}{q} \right| \right) \quad (2)$$

and

$$M(f) = \min_{(x,y) \in \mathbb{Z}^2 \setminus \{(0,0)\}} \frac{f(x,y)}{\sqrt{-\det f}}. \quad (3)$$

The monographs [1, 6, 10] and their bibliographies are excellent resources for that theory. (Often the Lagrange number is defined as the reciprocal value, $1/L(x)$.)

While the Lagrange number $L(x)$ and the Markov constant $M(f)$ are invariant under the actions of $GL_2(\mathbb{Z})$, the approximation number $C(x)$ is only invariant under the group of \mathbb{Z} -affine transformations

$$x \mapsto \pm x + n \quad (n \in \mathbb{Z}). \quad (4)$$

In fact, the irrational numbers with $C(x) > \frac{1}{3}$ classified by Gurwood are special representatives of the $GL_2(\mathbb{Z})$ -classes of Markov irrationals. In this article, we focus on the worst approximable rational numbers.

The connection between continued fractions and Diophantine approximation on the one hand, and hyperbolic geometry on the other hand is well established [4, 11, 20]. Both Markov forms and Markov irrationals correspond to geodesics in the modular torus [1, 7, 8, 16, 18, 31]: Markov forms correspond to simple closed geodesics, and Markov irrationals correspond to simple geodesics with one end in the cusp and the other end spiraling into a simple closed geodesic. The Lagrange number $L(x)$ and the Markov constant $M(f)$ correspond to distances between geodesics and the Ford circles interpreted as horocycles. This makes it possible to classify the Markov irrationals and Markov forms using purely geometric methods [32]. In this article, we take the same geometric approach to classify the worst approximable rational numbers.

Figure 1 illustrates the geometric interpretation of the approximation constant. The extended real line $\mathbb{R}P^1 = \mathbb{R} \cup \{\infty\}$ is the ideal boundary of the hyperbolic plane H^2 in the half-plane model. For an irrational number $x \in \mathbb{R} \setminus \mathbb{Q}$ and a bound $c > 0$, the approximation constant satisfies the inequality $C(x) \geq c$ if and only if x is visible from ∞ behind the Ford circles after they are scaled by $2c$. For a rational number, $x \in \mathbb{Q}$, the condition is that x is visible after the Ford circle at x itself is removed, or equivalently, that the highest point of the Ford circle at x is visible.

The classical approach to Diophantine approximation based on continued fractions can also be interpreted geometrically, because continued fractions encode the symbolic dynamics of geodesics in the Farey triangulation. But our geometric approach goes further. In effect, we trivialize the symbolic dynamics by considering not only one but all ideal triangulations of the modular torus.

2 Overview

2.1 Classification of the worst approximable rational numbers

The main result of this article is the classification of the worst approximable rational numbers in terms of *Markov fractions* (see Section 3.2) and their *companions* (see Section 3.3):

Theorem 2.1. *For a rational number $x \in \mathbb{Q}$, the following two statements are equivalent:*

- (i) $C(x) \geq \frac{1}{3}$
- (ii) *The number x is either a Markov fraction or a companion of a Markov fraction.*

Furthermore, $C(x) = \frac{1}{3}$ if and only if x is the first left or right companion of a Markov fraction.

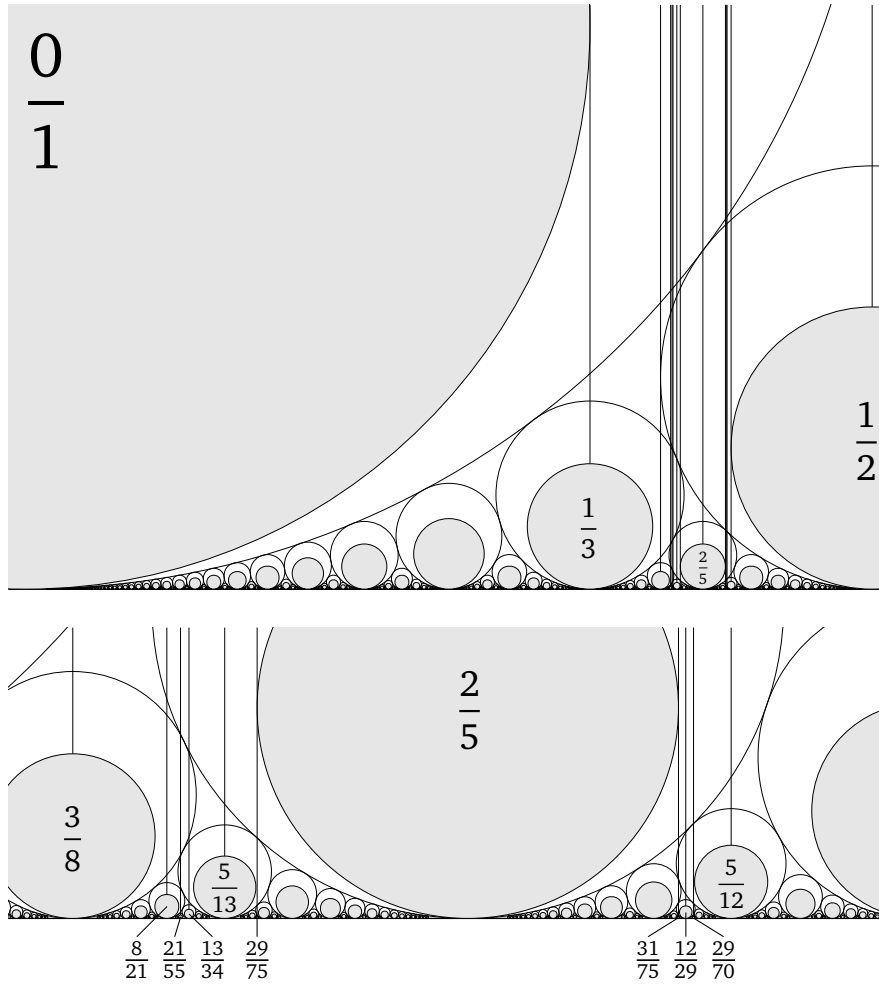


Figure 1: Ford circles scaled by $\frac{2}{3}$. Those whose highest point is visible from ∞ belong to rational numbers with approximation constant $\geq \frac{1}{3}$. A few of them are indicated in the figure (compare Figure 3 and Table 1). The bottom figure shows a detail of the top figure.

For the first companions of a Markov fraction, the approximation constant $C(x) = \frac{1}{3}$ is attained only by the associated Markov fraction, while for every rational number with $C(x) > \frac{1}{3}$, the approximation constant is attained by exactly two rational numbers (see Theorems 3.6 and 3.15).

The proof of Theorem 2.1 that is presented in Section 4.9 uses the characterization of Markov fractions and their companions in terms of geodesics in the modular torus (see Section 4).

Interest in classifying the worst approximable rational numbers was initially motivated by the *uniqueness conjecture for Markov numbers* [1, 24, 33]. This is the proposition — yet to be proved or refuted — that every Markov number is the

$$\begin{array}{ccc}
\frac{1}{1} & \frac{p_2}{q_2} & \boxed{\frac{p'}{q'}} \\
\hline
\frac{0}{1} & \frac{p_1}{q_1} &
\end{array}
\quad
\begin{array}{l}
p' = \frac{p_1 q_1 + p_2 q_2}{p_2 q_1 - p_1 q_2} \\
q' = \frac{q_1^2 + q_2^2}{p_2 q_1 - p_1 q_2}
\end{array}
\quad (5)$$

Figure 2: Root edge and generating rule for the tree of Markov fractions in $[0, 1]$, of which one half is shown in Figure 3

maximum of exactly one ordered Markov triple. Indeed, the uniqueness conjecture for Markov numbers is equivalent to the following uniqueness conjecture for Markov fractions:

Conjecture 2.2. *For each Markov number q , the interval $[0, \frac{1}{2}]$ contains at most one Markov fraction with denominator q .*

One may equivalently write “exactly one” instead of “at most one”, because the Markov fractions come in \mathbb{Z} -affine orbits and every Markov number appears among the denominators (see Section 3.2).

2.2 The forest of Markov fractions

The Markov fractions between zero and one are naturally associated with the faces of a plane binary tree with the root edge and generating rule shown in Figure 2 (see Lemma 3.8). For example, the first branching after the root edge produces the Markov fraction $\frac{1}{2}$. At each node, the numbers p' and q' obtained by equations (5) are coprime integers, so the Markov fraction $\frac{p'}{q'}$ is reduced.

Figure 3 shows the first few levels of the subtree containing the Markov fractions in the interval $[0, \frac{1}{2}]$. There is a symmetric subtree containing the Markov fractions in $[\frac{1}{2}, 1]$, obtained by a reflection and replacing each Markov fraction x with $1 - x$. Likewise, the Markov fractions $x + n$ in any other integer interval $[n, n + 1]$ are arranged in a similar tree, and all these trees form a plane binary forest. The generating rule is the same for all trees, and the root edges are infinite parallel rays separating faces associated with consecutive integers (see Figure 4).

At each node in the forest, the three Markov fractions form a *rational Markov triple* $(\frac{p_1}{q_1}, \frac{p'}{q'}, \frac{p_2}{q_2})$ which is *centered* (see Definitions 3.1 and 3.4). Conversely, all centered rational Markov triples arise in this way, except for the integer triples $(n - 1, n, n + 1) \in \mathbb{Z}^3$ which correspond to pairs of neighboring root edges.

2.3 Limits of infinite paths in the forest

The forest structure of the set of Markov fractions is useful to study the set of its accumulation points. But first note that every accumulation point of the set of

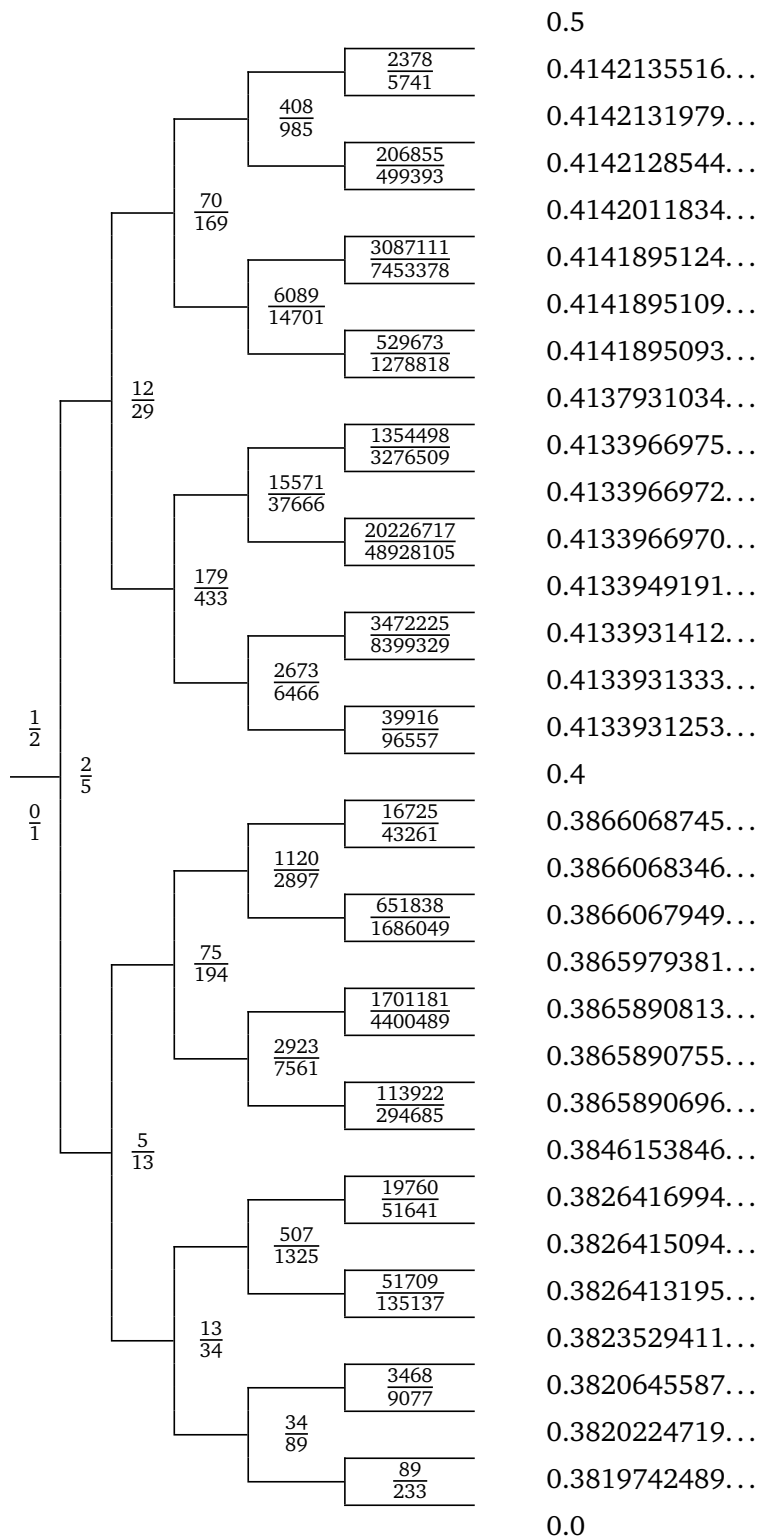


Figure 3: Markov fractions in the interval $[0, \frac{1}{2}]$. Numerical values are shown in the right column.

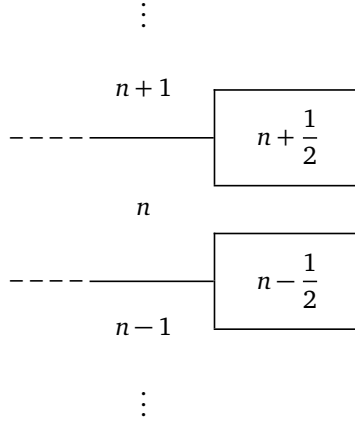


Figure 4: Roots of the forest of Markov fractions

Markov fractions is irrational. Indeed for $\frac{a}{b} \in \mathbb{Q}$ and a Markov fraction $\frac{p}{q} \neq \frac{a}{b}$, we have $|\frac{p}{q} - \frac{a}{b}| > \frac{b^2}{3}$, so $\frac{a}{b}$ is not an accumulation point.

Now consider infinite paths in the tree of Markov fractions between 0 and 1, starting at the root edge. Each path corresponds to a sequence of Markov fractions with increasing denominators, which converges to an irrational number x with Lagrange number $L(x) \geq \frac{1}{3}$.

For example, always taking the lower branch in Figure 3 generates the sequence

$$\frac{1}{2}, \frac{2}{5}, \frac{5}{13}, \frac{13}{34}, \dots$$

which converges to

$$\phi^{-2} = \frac{1}{2}(3 - \sqrt{5}) = 2 - \phi,$$

with $\phi = \frac{1}{2}(1 + \sqrt{5})$, the golden ratio. This is a Markov irrational with Lagrange number $L(2 - \phi) = L(\phi) = \frac{1}{\sqrt{5}} > \frac{1}{3}$.

Always taking the upper branch in Figure 3 generates the sequence

$$\frac{2}{5}, \frac{12}{29}, \frac{70}{169}, \frac{408}{985}, \dots$$

with limit $-1 + \sqrt{2}$. This is another Markov irrational, with Lagrange number $L(-1 + \sqrt{2}) = L(\sqrt{2}) = \frac{1}{\sqrt{8}} > \frac{1}{3}$.

For these two examples, the limits represent the two worst approximable classes of irrational numbers. But there are only a countable number of $PGL_2(\mathbb{Z})$ -classes of Markov irrationals and an uncountable number of paths in an infinite binary tree, so these two examples are exceptional. In fact, the limit x is a Markov irrational if the path turns always left or always right except for finitely many branchings. If, on the other hand, there are infinitely many left turns and

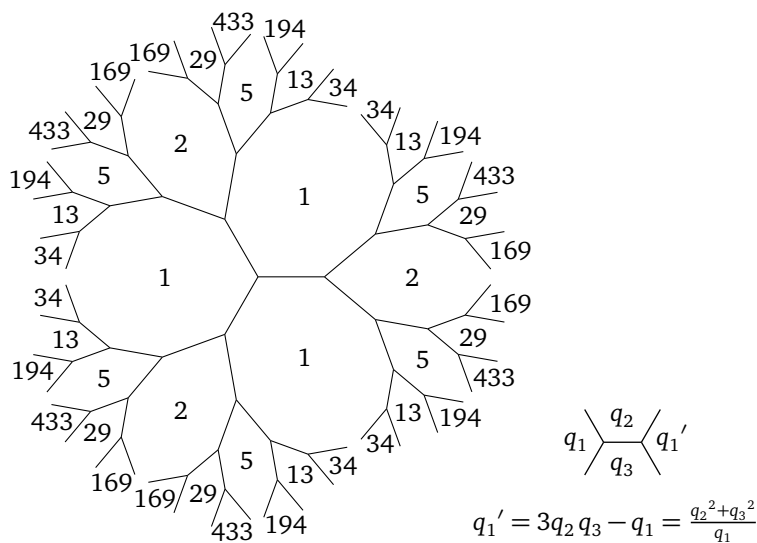


Figure 5: The tree of Markov numbers and its generating rule

infinitely many right turns, then the limit has Lagrange number $L(x) = \frac{1}{3}$. Before we come back to this in Section 2.5, let us use the Stern–Brocot tree to label Markov fractions.

2.4 Labeling the Markov fractions in the unit interval

The denominators of Markov fractions are Markov numbers. If we take the subtree of Markov fractions in the interval $[0, \frac{1}{2}]$ shown in Figure 3 and replace the fractions by their denominators alone, we obtain one of the six symmetric subtrees of the tree of Markov numbers shown in Figure 5. The combinatorial isomorphism with the Stern–Brocot tree leads to the customary labeling of Markov numbers by the rational numbers in the interval $[0, 1]$. If we do not forget about the numerators of the Markov fractions, we obtain a labeling of the Markov fractions in the interval $[0, \frac{1}{2}]$. For our purposes, it makes sense to extend the Stern–Brocot tree to contain all non-negative rational numbers and $\frac{1}{0} = \infty$. That is, we consider the rooted trivalent plane tree with the following root edge and generating rule:

$$\begin{array}{c} \frac{1}{0} \\ \hline \frac{0}{1} \end{array}
 \qquad
 \begin{array}{c} \frac{p_2}{q_2} \\ \hline \frac{p_1}{q_1} \end{array}
 \begin{array}{|c|} \hline \frac{p_1 + p_2}{q_1 + q_2} \\ \hline \end{array}$$

The combinatorial isomorphism of rooted plane trees leads to a bijection

$$\begin{aligned} \mu : \mathbb{Q}_{\geq 0} \cup \{\infty\} &\longrightarrow \{\text{Markov fractions}\} \cap [0, 1] \\ \frac{n}{m} &\longmapsto \mu_{\frac{n}{m}}. \end{aligned} \quad (6)$$

The symmetries of the (extended) Stern-Brocot tree and the tree of Markov fractions in $[0, 1]$ lead to the functional equation $\mu_{\frac{n}{m}} + \mu_{\frac{m}{n}} = 1$. For example:

$\frac{n}{m}$	$\frac{0}{1}$	$\frac{1}{3}$	$\frac{1}{2}$	$\frac{2}{3}$	$\frac{1}{1}$	$\frac{3}{2}$	$\frac{2}{1}$	$\frac{3}{1}$	$\frac{1}{0}$
$\mu_{\frac{n}{m}}$	$\frac{0}{1}$	$\frac{5}{13}$	$\frac{2}{5}$	$\frac{12}{29}$	$\frac{1}{2}$	$\frac{17}{29}$	$\frac{3}{5}$	$\frac{8}{13}$	$\frac{1}{1}$

The same correspondence μ also arises from the construction involving triangle paths in the Eisenstein lattice explained in Section 2.6.

2.5 Limits of infinite paths (continued)

The combinatorial isomorphism between the (extended) Stern–Brocot tree and the tree of Markov fractions in the interval $[0, 1]$ extends to a bijection between infinite paths starting at the root edges of either tree, respectively.

Each infinite path in the Stern–Brocot tree generates a sequence of nonnegative rational numbers that converges to a finite limit or diverges properly to ∞ . The limit of a path with infinitely many left turns and infinitely many right turns is irrational, and each positive irrational number is the limit for precisely one such path. Indeed, the sequence of partial denominators of the continued fraction expansion is the run-length encoding of the sequence of left and right turns. On the other hand, an infinite path with only finitely many left or finitely many right turns has a rational limit, and every positive rational number is the limit for two such paths. The two corresponding paths in the tree of Markov fractions have different but $PGL_2(\mathbb{Z})$ -equivalent Markov irrationals as limits. Thus, the correspondence of infinite paths defines a map

$$\widehat{\mu} : \mathbb{R}_{\geq 0} \cup \{\infty\} \longrightarrow \{PGL_2(\mathbb{Z})\text{-classes of real numbers with } L \geq \frac{1}{3}\}.$$

If x is rational, $\widehat{\mu}(x)$ is a class of Markov irrationals. Otherwise, $\widehat{\mu}(x)$ is a class of irrationals with Lagrange number $= \frac{1}{3}$. It is not difficult to see that the restriction of $\widehat{\mu}$ to $\mathbb{Q} \cap [0, 1]$ is a bijection onto the set of equivalence classes of Markov irrationals. What about the restriction of $\widehat{\mu}$ to $[0, 1] \setminus \mathbb{Q}$? The following two questions seem to be open:

Question 2.3. Is every irrational number x with Lagrange number $L(x) = \frac{1}{3}$ equivalent to the limit of some infinite path in the tree of Markov fractions between 0 and 1?

Question 2.4. Do two different infinite paths exist in the subtree containing all Markov fractions between 0 and $\frac{1}{2}$ (see Figure 3) such that their limits are $PGL_2(\mathbb{Z})$ -equivalent with Lagrange number $L = \frac{1}{3}$?

2.6 Triangle paths for Markov fractions

The Markov fractions $\mu_{\frac{n}{m}}$ can be found by a Fibonacci-like recursion with Farey addition along triangle paths (see Figure 6). The following theorem defines this construction more precisely, extending the snake graph construction for Markov numbers [27].

Theorem 2.5 (Triangle paths for Markov fractions). *Let $m \geq 0$ and $n \geq 0$ be coprime integers, let $z_{m,n} = m + n\omega$ with $\omega = \frac{1}{2}(1 + i\sqrt{3})$, and let α be the oriented straight line segment from 0 to $z_{m,n}$. Let $\tau_0 = [0, 1, \omega]$, and unless (m, n) equals $(1, 0)$ or $(0, 1)$, let*

$$\tau_1 = [1, \omega, 1 + \omega], \quad \dots, \quad \tau_N = [z_{m,n} - 1, z_{m,n} - \omega, z_{m,n}]$$

be the finite sequence of triangles in the Eisenstein lattice $\mathbb{Z} + \omega\mathbb{Z}$ that α intersects after τ_0 . Recursively label the vertices of these triangles as follows:

- Label the vertices 0, 1, and ω of τ_0 with $\frac{1}{0}$, $\frac{0}{1}$, and $\frac{1}{1}$, respectively.
- If the vertices of $\tau_0, \dots, \tau_{j-1}$ are already labeled, label the remaining vertex of triangle τ_j with $\frac{p_1+p_2}{q_1+q_2}$, where $\frac{p_1}{q_1}$ and $\frac{p_2}{q_2}$ are the labels at the vertices shared with triangle τ_{j-1} .

Then the label at $z_{m,n}$ is the Markov fraction $\mu_{\frac{n}{m}}$.

In Section 4.10, this construction is derived by following geodesics in the Farey triangulation.

Remark 2.6 (Triangle paths and hyperbolic geodesics). In Figure 6, the point 0 (labeled $\frac{1}{0}$) is connected to the points $z_{m,n}$ (labeled with the Markov fractions $\mu_{\frac{n}{m}}$) not by straight line segments as described in Theorem 2.5, but by polygonal curves that are determined as follows. Define a hyperbolic metric on each triangle strip by equipping each triangle with the hyperbolic Beltrami–Klein metric defined by its circumcircle [3, Ch. 5.1]. In this metric, the polygonal curves shown in Figures 6 and 8 are hyperbolic geodesics connecting their ideal endpoints. We use this construction because it works equally well for companions (see Figure 8), whereas the straight line segments would have vertices in their interior. More importantly, Markov fractions and their companions correspond to certain geodesics in the modular torus with both ends in the cusp, and the polygonal curves shown in Figures 6 and 8 are natural representations of these geodesics in the following sense: The canonical ideal triangulation of the modular torus induces a euclidean metric on it [12], and if one uses this euclidean metric to lift the hyperbolic geodesics to the euclidean plane, one obtains the polygonal curves shown in the figures.

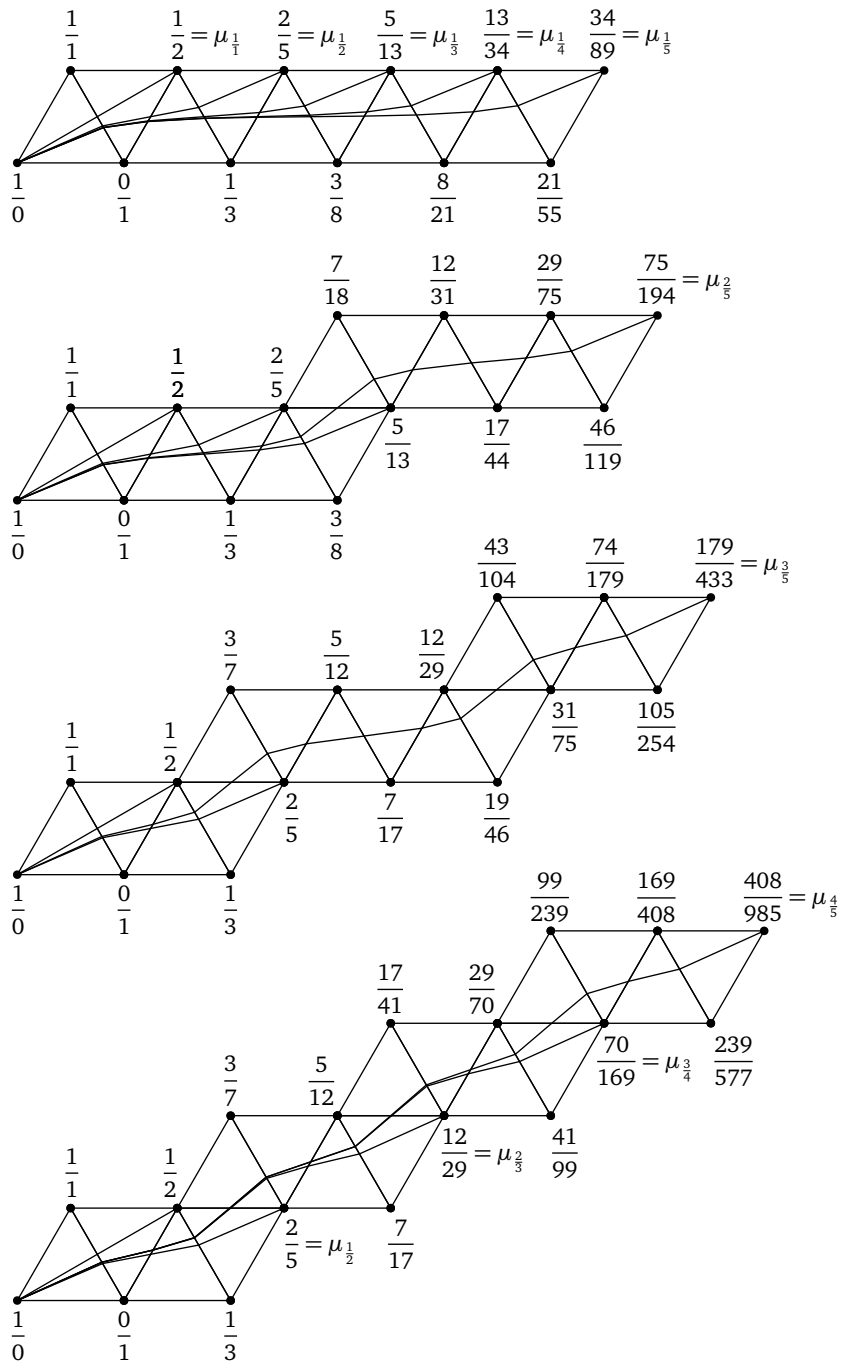


Figure 6: Triangle paths of the Markov fractions $\mu_{\frac{n}{m}}$ with $1 \leq n < m \leq 5$.

2.7 Companions of Markov fractions

Table 1 lists the first few *right companions*, $\gamma_2^+(\frac{p}{q}), \gamma_3^+(\frac{p}{q}), \dots$, for each Markov fraction $\frac{p}{q} = \gamma_1^+(\frac{p}{q})$ with denominator $q < 1000$ (see Definition 3.9). The corresponding *left companions* $\gamma_k^-(\frac{p}{q})$ are symmetrically located:

$$\gamma_k^-(\frac{p}{q}) + \gamma_k^+(\frac{p}{q}) = 2\frac{p}{q}. \quad (7)$$

The sequences of right and left companions converge to $\frac{p}{q} \pm \delta_q$, respectively, with

$$\delta_q = \frac{3}{2} - \sqrt{\frac{9}{4} - \frac{1}{q^2}}. \quad (8)$$

The closed interval

$$I_{\frac{p}{q}} = \left[\frac{p}{q} - \delta_q, \frac{p}{q} + \delta_q \right] \quad (9)$$

contains all companions of $\frac{p}{q}$, but neither any other Markov fractions nor their companions, but the endpoints of the interval are limit points of the set of Markov fractions (see Lemma 4.16).

Figure 7 indicates a striking self-similarity in the arrangement of Markov fractions and their companions.

2.8 Triangle paths for companions

The left and right companions of a Markov fraction can also be found by a Fibonacci-like recursion along triangle paths (see Figure 8). Roughly speaking, while the Markov fractions are obtained from triangle paths of primitive lattice vectors, the companions are obtained from triangle paths of imprimitive lattice vectors. To avoid lattice points in their interior, the paths are bent slightly to the left or to the right, which leads to right or left companions, respectively. More precisely:

Theorem 2.7 (Triangle paths for companions). *With $m, n, \omega, z_{m,n}$, and α as in Theorem 2.5, let k be an integer ≥ 2 , so that the oriented line segment $k\alpha$ from 0 to $kz_{m,n} = z_{km, kn}$ contains $k-1$ vertices of the Eisenstein lattice in its interior. Bend this line segment slightly to the left or to the right while keeping the endpoints fixed to obtain an oriented curve β^+ or β^- , respectively, that avoids lattice points in the interior. Or, to be more precise and more definite, let β^\pm be the curve*

$$\beta^\pm : [0, 1] \rightarrow \mathbb{C}, \quad \beta^\pm(t) = (t \pm i\epsilon t(1-t))kz_{m,n},$$

where $\epsilon > 0$ is chosen small enough so that there are no lattice points between the line segment $k\alpha$ and β^\pm or in the interior of β^\pm . As in Theorem 2.5, label the vertices 0, 1, and ω with $\frac{1}{0}$, $\frac{0}{1}$, and $\frac{1}{1}$, respectively, and label the vertices of the triangles $\tilde{\tau}_0^\pm, \dots, \tilde{\tau}_N^\pm$ crossed by β^\pm recursively, so that in each triangle of the sequence the as yet unlabeled vertex is labeled with the Farey sum of the already labeled vertices.

Then the label at $kz_{m,n}$ is $\gamma_k^\pm(\frac{p}{q})$, the $(k-1)$ st left or right companion of $\frac{p}{q} = \mu_{\frac{p}{m}}$.

$\frac{p}{q} = \gamma_1^+\left(\frac{p}{q}\right), \gamma_2^+\left(\frac{p}{q}\right), \gamma_3^+\left(\frac{p}{q}\right), \dots$	$\longrightarrow \lim \gamma_k\left(\frac{p}{q}\right)$
$\frac{0}{1}, \frac{1}{3}, \frac{3}{8}, \frac{8}{21}, \frac{21}{55}, \frac{55}{144}, \frac{144}{377}, \frac{377}{987}, \frac{987}{2584}, \dots$	$\longrightarrow \frac{1}{2}(3 - \sqrt{5})$
$\frac{1}{2}, \frac{7}{12}, \frac{41}{70}, \frac{239}{408}, \frac{1393}{2378}, \frac{8119}{13860}, \frac{47321}{80782}, \dots$	$\longrightarrow 2 - \sqrt{2}$
$\frac{2}{5}, \frac{31}{75}, \frac{463}{1120}, \frac{6914}{16725}, \frac{103247}{249755}, \frac{1541791}{3729600}, \dots$	$\longrightarrow \frac{1}{10}(19 - \sqrt{221})$
$\frac{5}{13}, \frac{196}{507}, \frac{7639}{19760}, \frac{297725}{770133}, \frac{11603636}{30015427}, \dots$	$\longrightarrow \frac{1}{26}(49 - \sqrt{1517})$
$\frac{12}{29}, \frac{1045}{2523}, \frac{90903}{219472}, \frac{7907516}{19091541}, \frac{687862989}{1660744595}, \dots$	$\longrightarrow \frac{1}{58}(111 - \sqrt{7565})$
$\frac{13}{34}, \frac{1327}{3468}, \frac{135341}{353702}, \frac{13803455}{36074136}, \frac{1407817069}{3679208170}, \dots$	$\longrightarrow \frac{1}{17}(32 - \sqrt{650})$
$\frac{34}{89}, \frac{9079}{23763}, \frac{2424059}{6344632}, \frac{647214674}{1693992981}, \dots$	$\longrightarrow \frac{1}{178}(335 - \sqrt{71285})$
$\frac{70}{169}, \frac{35491}{85683}, \frac{17993867}{43441112}, \frac{9122855078}{22024558101}, \dots$	$\longrightarrow \frac{1}{338}(647 - \sqrt{257045})$
$\frac{75}{194}, \frac{43651}{112908}, \frac{25404807}{65712262}, \frac{14785554023}{38244423576}, \dots$	$\longrightarrow \frac{1}{97}(183 - \sqrt{21170})$
$\frac{89}{233}, \frac{62212}{162867}, \frac{43486099}{113843800}, \frac{30396720989}{79576653333}, \dots$	$\longrightarrow \frac{1}{466}(877 - \sqrt{488597})$
$\frac{179}{433}, \frac{232522}{562467}, \frac{302045899}{730644200}, \frac{392357390279}{949106253333}, \dots$	$\longrightarrow \frac{1}{866}(1657 - \sqrt{1687397})$
$\frac{233}{610}, \frac{426391}{1116300}, \frac{780295297}{2042828390}, \frac{1427939967119}{3738374837400}, \dots$	$\longrightarrow \frac{1}{305}(574 - \sqrt{209306})$
$\frac{408}{985}, \frac{1205641}{2910675}, \frac{3562668747}{8601043640}, \frac{10527684941744}{25416081045525}, \dots$	$\longrightarrow \frac{1}{1970}(3771 - \sqrt{8732021})$

Table 1. The first few right companions, $\gamma_2^+, \gamma_3^+, \dots$, of the Markov fractions $\frac{p}{q}$ with denominator $q < 1000$. The limits are Markov irrationalities, i.e., irrational numbers x with Lagrange number $L(x) > \frac{1}{3}$. The fractions in the first row are equal to F_{2k-2}/F_{2k} , and the denominators in the second row are equal to the Pell numbers P_{2k} (see Remark 3.14 and compare Figure 3).

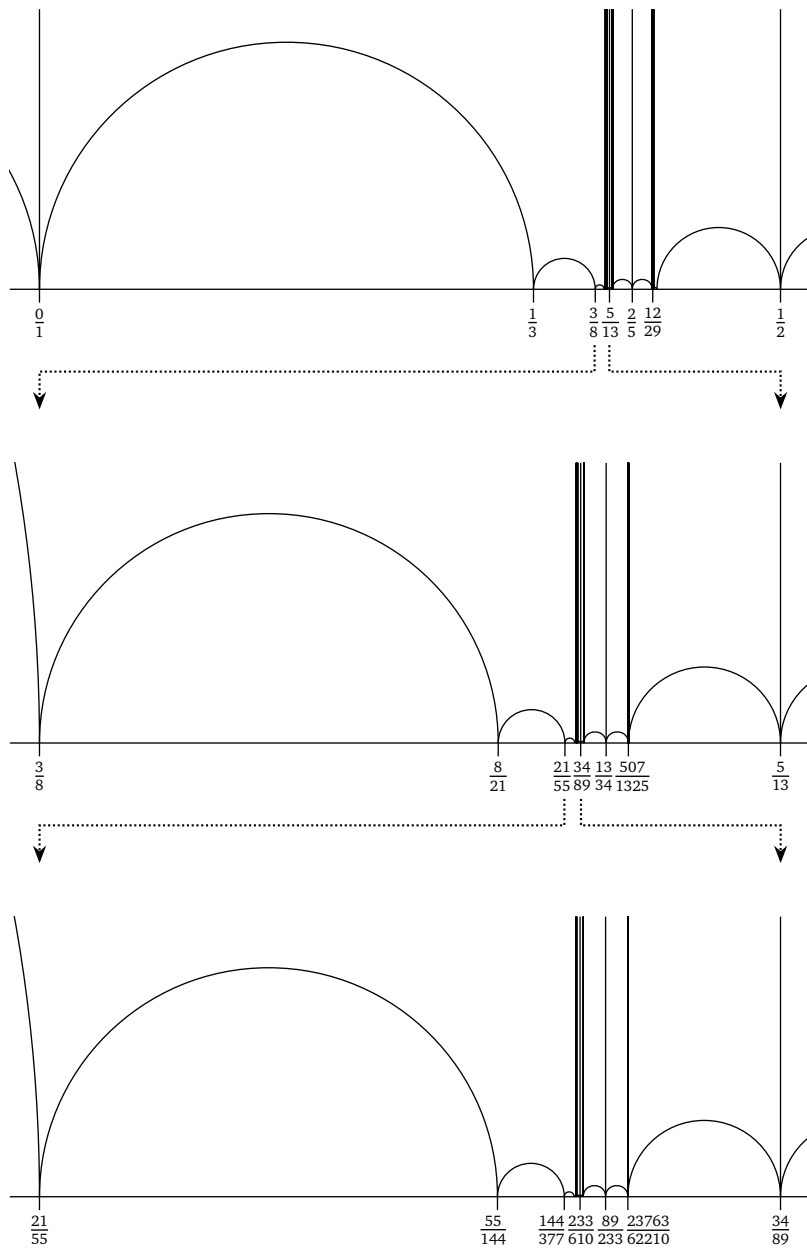


Figure 7: Markov fractions and their companions. Markov fractions are marked by vertical lines and connected to their companions by semicircles. The only companions that are visually discernible at the scales of these figures are the first six right companions of $\frac{0}{1}$ (see Table 1). The vertical lines and semicircles project to simple geodesics in the modular torus with both ends in the cusp.

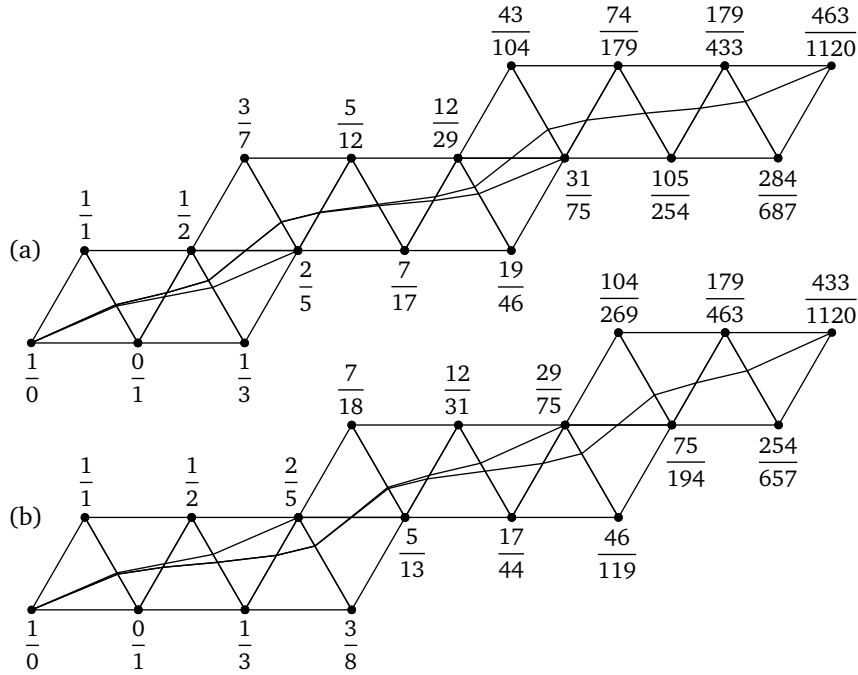


Figure 8: (a) Triangle paths for $\mu_{\frac{1}{2}} = \frac{2}{5}$ and the first and second right companions $\gamma_2^+(\frac{2}{5}) = \frac{31}{75}$ and $\gamma_3^+(\frac{2}{5}) = \frac{463}{1120}$. (b) Same for the first and second left companions $\gamma_2^-(\frac{2}{5}) = \frac{29}{75}$ and $\gamma_3^-(\frac{2}{5}) = \frac{433}{1120}$.

Like the analogous construction for Markov fractions (see Theorem 2.5), this is derived by following geodesics in the Farey triangulation (see Section 4.10).

2.9 Hyperbolic geometry

In the upper half-space model of the the hyperbolic plane,

$$H^2 = \{z \in \mathbb{C} \mid \text{Im } z > 0\} \quad \text{with metric} \quad ds = \frac{|dz|}{\text{Im } z},$$

we associate a horocycle $h(p, q)$ with every pair (p, q) of real numbers, not both zero:

- If $q \neq 0$, $h(p, q)$ is the horocycle centered at $\frac{p}{q}$ with euclidean diameter $\frac{1}{q^2}$.
- $h(p, 0)$ is the horizontal horocycle centered at ∞ with equation $\text{Im } z = p^2$.

This establishes a $PSL_2(\mathbb{R})$ -equivariant bijection between the space

$$(\mathbb{R}^2 \setminus \{(0, 0)\}) / \{\pm 1\}$$

of *lax vectors* (in Conway's terminology [9]) and the space of horocycles in the hyperbolic plane [13, p. 665], y[32, Ch. 5].

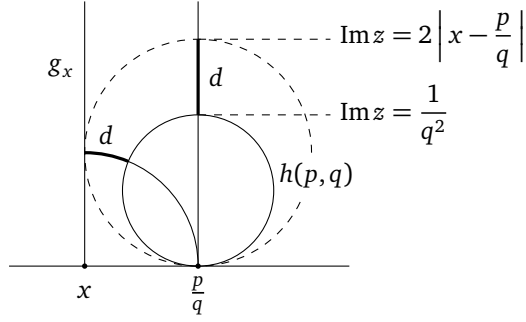


Figure 9: Signed distance $d = d(g_x, h(p, q))$ between the vertical geodesic g_x and the horocycle $h(p, q)$.

The following observation translates between Diophantine approximation and hyperbolic geometry:

Lemma 2.8 ([32, Proposition 8.1]). *The signed distance $d(g_x, h(p, q))$ of the vertical geodesic g_x in H^2 joining $x \in \mathbb{R}$ and ∞ and a horocycle $h(p, q)$ with $q \neq 0$ and $\frac{p}{q} \neq x$ satisfies*

$$d(g_x, h(p, q)) = \log \left(2q^2 \left| x - \frac{p}{q} \right| \right). \quad (10)$$

Proof. See Figure 9. □

If p and q are coprime integers, then the horocycle $h(p, q)$ is a *Ford circle*. The previous lemma relates the approximation number $C(x)$ to the minimal signed distance between the geodesic g_x and a Ford circle $h(p, q)$ not centered at either ∞ or x (see also Figure 1):

Corollary 2.9. *For $x \in \mathbb{R}$,*

$$\log(2C(x)) = \inf_{\frac{p}{q} \in \mathbb{Q} \setminus \{x\}} d(g_x, h(p, q)). \quad (11)$$

In particular, the following two statements are equivalent:

- (i) $C(x) \geq \frac{1}{3}$
- (ii) For all Ford circles $h(p, q)$ with $\frac{p}{q} \in \mathbb{Q} \setminus \{x\}$,

$$d(g_x, h(p, q)) \geq \log \frac{2}{3}. \quad (12)$$

The hyperbolic plane H^2 is the universal cover of the modular torus M (see Section 4), and the Ford circles project to the boundary of the maximal cusp neighborhood in the modular torus. The geometric proof of the classification Theorem 2.1 for worst approximable rational numbers in Section 4.9 also proves the following classification theorem of geodesics in M that have both ends in the cusp but otherwise stay furthest away from the cusp:

Theorem 2.10. *Let g be a geodesic in the modular torus M with both ends in the cusp. Then the following statements are equivalent:*

- (i) *Away from the ends, the signed distance between g and the cusp is $\geq \log \frac{2}{3}$.*
- (ii) *g does not intersect all simple closed geodesics in M .*
- (iii) *g does not intersect all simple geodesics in M with both ends in the cusp.*

If one and hence all of these conditions hold, then either

- (a) *g is a simple geodesic. In this case there is a unique simple closed geodesic that does not intersect g , and infinitely many simple geodesics with both ends in the cusp that do not intersect g .*
- (b) *g has self-intersections, and then there are a unique closed geodesic c in M and a unique simple geodesic \tilde{g} in M with both ends in the cusp that do not intersect g .*

In case (a), the geodesic g in M is the projection of a vertical geodesic g_x in H^2 for some Markov fraction x . In case (b), the geodesic g in M is the projection of a vertical geodesic g_x in H^2 for some companion x of a Markov fraction \tilde{x} , and the geodesic \tilde{g} in M is the projection of the vertical geodesic $g_{\tilde{x}}$ in H^2 .

3 The algebraic point of view

This section treats the two types of worst approximable rational numbers, the Markov fractions and their companions, from the algebraic point of view. Geometrically minded readers may want to look at Section 4 first, which provides a complementary geometric point of view.

3.1 Markov numbers and Markov triples

For reference and to fix notation, we begin with a brief review of some basic definitions and facts about Markov numbers and Markov triples [1, 6, 10].

A *Markov triple* (q_1, q_2, q_3) is a positive integer solution of Markov's equation

$$x^2 + y^2 + z^2 = 3xyz. \quad (13)$$

Equivalently, a triple of positive integers $(q_1, q_2, q_3) \in (\mathbb{Z}_{>0})^3$ is a Markov triple if and only if

$$\frac{q_1}{q_2 q_3} + \frac{q_2}{q_3 q_1} + \frac{q_3}{q_1 q_2} = 3. \quad (14)$$

A *Markov number* is a positive integer that is an element of some Markov triple. For example, $(5, 1, 2)$ and $(1, 5, 2)$ are two of the six Markov triples containing the Markov numbers 1, 2, and 5.

Since Markov's equation (13) is quadratic in each variable, there are two solutions for each variable if the other two variables are fixed. Thus, if (q_1, q_2, q_3) is a Markov triple, then so are its *neighbors*

$$(q'_1, q_2, q_3), \quad (q_1, q'_2, q_3), \quad (q_1, q_2, q'_3),$$

where the q'_i are determined by Vieta's formulas for quadratic polynomials, i.e.,

$$q'_i = \frac{q_j^2 + q_k^2}{q_i} = 3q_j q_k - q_i \quad (15)$$

with $\{i, j, k\} = \{1, 2, 3\}$. This neighbor relation turns the set of Markov triples into a plane binary tree. The Markov numbers correspond to the regions into which the tree separates the plane (see Figure 5).

The root Markov triple $(1, 1, 1)$ and its neighbors $(2, 1, 1)$, $(1, 2, 1)$, and $(1, 1, 2)$ are called *singular*. All other Markov triples are called *non-singular* and consist of three different Markov numbers. For each Markov triple, there is a unique path to the root. At each step along this path, the largest Markov number of the triple is replaced according to the rule (15).

3.2 Markov fractions and rational Markov triples

Markov fractions are one of the two types of worst approximable rational numbers (see Theorems 2.1 and 3.6). Like the Markov numbers, Markov fractions are defined in terms of triples:

Definition 3.1. (i) A triple of rational numbers (x_1, x_2, x_3) is a *rational Markov triple* if $x_k = \frac{p_k}{q_k}$ for some Markov triple (q_1, q_2, q_3) and some integers p_1, p_2, p_3 satisfying the equations

$$p_2 q_1 - p_1 q_2 = q_3, \quad (16)$$

$$p_3 q_2 - p_2 q_3 = q_1. \quad (17)$$

(ii) A *Markov fraction* is a rational number x_k that is an element of some rational Markov triple (x_1, x_2, x_3) .

A rational Markov triple (x_1, x_2, x_3) is strictly increasing,

$$x_1 < x_2 < x_3,$$

because Markov numbers are positive and equations (16) and (17) are equivalent to

$$\frac{p_2}{q_2} - \frac{p_1}{q_1} = \frac{q_3}{q_1 q_2} \quad \text{and} \quad \frac{p_3}{q_3} - \frac{p_2}{q_2} = \frac{q_1}{q_2 q_3}. \quad (18)$$

Equations (14), (15), and (18) also yield the relation

$$p_3 q_1 - p_1 q_3 = q'_2 \quad (19)$$

with q'_2 defined by (15), which will be used in the proof of Lemma 3.2.

Since the Markov numbers q_k of a Markov triple (q_1, q_2, q_3) are pairwise coprime, equations (16) and (17) imply that each pair p_k, q_k is also coprime, so the fractions $\frac{p_k}{q_k}$ are reduced. This means that the Markov triple (q_1, q_2, q_3) in

Definition 3.1 is uniquely determined by the rational Markov triple (x_1, x_2, x_3) . Further, if (x_1, x_2, x_3) is a rational Markov triple, then for every $n \in \mathbb{Z}$,

$$(x_1 + n, x_2 + n, x_3 + n)$$

is also a rational Markov triple with the same Markov triple (q_1, q_2, q_3) of denominators, and all rational Markov triples with this denominator triple are obtained in this way. Since $(-x_3, -x_2, -x_1)$ is also a rational Markov triple, the group of \mathbb{Z} -affine transformations (4) acts on the set of rational Markov triples, and hence on the set of Markov fractions.

There is another \mathbb{Z} -action on the set of rational Markov triples: Using equations (14) and (18), it is easy to check that

$$(x_3 - 3, x_1, x_2) \quad \text{and} \quad (x_2, x_3, x_1 + 3) \quad (20)$$

are also rational Markov triples, with cyclically permuted denominators. So the action of the cyclic permutation group $A_3 \simeq \mathbb{Z}_3$ on the set of Markov triples (q_1, q_2, q_3) lifts to a free action of \mathbb{Z} on the set of rational Markov triples $(\frac{p_1}{q_1}, \frac{p_2}{q_2}, \frac{p_3}{q_3})$. Accordingly, the tree of Markov numbers (see Figure 5) corresponds to the forest of Markov fractions constructed in Lemma 3.8, a subtree of which is shown in Figure 3.

To see that there exists a rational Markov triple $(\frac{p_1}{q_1}, \frac{p_2}{q_2}, \frac{p_3}{q_3})$ for each Markov triple (q_1, q_2, q_3) , note that the coprimality of Markov triples implies the existence of p_1 and p_2 satisfying (16) (and p_2 and p_3 satisfying (17), and p_1 and p_3 satisfying (19)). By the following lemma, there exists a suitable p_3 (or p_1 or p_2 , respectively) to complete the rational Markov triple.

Lemma 3.2 (Completion of rational Markov triples). *Let (q_1, q_2, q_3) be a Markov triple.*

(i) *If $p_1, p_2 \in \mathbb{Z}$ satisfy equation (16), then $\frac{p_2^2 + 1}{q_2} \in \mathbb{Z}$, and*

$$p_3 := q_1 \cdot \frac{p_2^2 + 1}{q_2} - p_1 p_2 \quad (21)$$

satisfies equation (17).

(ii) *If $p_2, p_3 \in \mathbb{Z}$ satisfy equation (17), then $\frac{p_2^2 + 1}{q_2} \in \mathbb{Z}$, and*

$$p_1 := p_2 p_3 - q_3 \cdot \frac{p_2^2 + 1}{q_2} \quad (22)$$

satisfies equation (16).

(iii) *If $p_1, p_3 \in \mathbb{Z}$ satisfy equation (19), then*

$$p_2 := \frac{p_1 q_1 + p_3 q_3}{q_2'} \quad (23)$$

is an integer and satisfies equations (16) and (17).

In any case, therefore, $(\frac{p_1}{q_1}, \frac{p_2}{q_2}, \frac{p_3}{q_3})$ is a rational Markov triple, which is, moreover, uniquely determined by $(\frac{p_1}{q_1}, \frac{p_2}{q_2})$, $(\frac{p_2}{q_2}, \frac{p_3}{q_3})$, or $(\frac{p_1}{q_1}, \frac{p_3}{q_3})$, respectively.

For a proof see Section 3.2.1. The integrality $\frac{p_2^2+1}{q_2}$ implies the following necessary condition for Markov numbers, which is well known [1, Lemma 3.14] and was proved in a similar way [30, p. 196]:

Corollary 3.3. *If q is a Markov number, then -1 is a quadratic residue modulo q .*

It will be useful to extend the distinction between singular and non-singular Markov triples (see Section 3.1) to rational Markov triples, and to have a special term to single out the rational Markov triples with denominators $(1, 1, 1)$. Also, since we are especially interested in rational Markov triples in which the second denominator is largest (see Theorem 3.6), it makes sense to introduce a special term for those, too:

Definition 3.4. A rational Markov triple $(\frac{p_1}{q_1}, \frac{p_2}{q_2}, \frac{p_3}{q_3})$ is called

- *singular* if the Markov triple (q_1, q_2, q_3) is singular, i.e., $\{q_1, q_2, q_3\} \subset \{1, 2\}$,
- *integral* if $q_1 = q_2 = q_3 = 1$, and
- *centered* if

$$q_2 \geq \max\{q_1, q_3\}. \quad (24)$$

Integral rational Markov triples are of the form $(n-1, n, n+1)$ with $n \in \mathbb{Z}$. They are integral, centered, and the only centered rational Markov triples for which (24) is satisfied with equality. All non-integral singular Markov triple have one of the forms $(n, n + \frac{1}{2}, n+1)$, $(n-2, n, n + \frac{1}{2})$ or $(n - \frac{1}{2}, n, n+2)$ for $n \in \mathbb{Z}$, of which precisely those of the first form are centered.

Remark 3.5. The notion of a centered rational Markov triple is closely related to Rockett & Szűsz's concept of a *complete Markov triple* [28, p. 103]: If $(\frac{p_1}{q_1}, \frac{p_2}{q_2}, \frac{p_3}{q_3})$ is a centered rational Markov triple with $\frac{p_k}{q_k} \in [0, \frac{1}{2}]$ then $(q_2, p_2; q_1, p_1; q_3, p_3)$ is a complete Markov triple. Compare also Figure 3 with [28, p. 105]. However, the idea to interpret the pairs (q_i, p_i) as rational numbers $\frac{p_i}{q_i}$ does not seem to be obvious in the context of [28].

We can now state the main result about the approximation constant of a Markov fraction, and the best approximating rationals that achieve it, as follows:

Theorem 3.6 (Best approximants of Markov fractions). *(i) Every Markov fraction is the middle element of a unique centered rational Markov triple.*

(ii) If $(\frac{p_1}{q_1}, \frac{p_2}{q_2}, \frac{p_3}{q_3})$ is a centered rational Markov triple, then the best approximants of $\frac{p_2}{q_2}$ are precisely $\frac{p_1}{q_1}$ and $\frac{p_3}{q_3}$, i.e.,

$$C\left(\frac{p_2}{q_2}\right) = q_1^2 \cdot \left(\frac{p_2}{q_2} - \frac{p_1}{q_1}\right) = q_3^2 \cdot \left(\frac{p_3}{q_3} - \frac{p_2}{q_2}\right),$$

and for every rational number $\frac{a}{b}$ not contained in the triple,

$$C\left(\frac{p_2}{q_2}\right) < b^2 \cdot \left| \frac{p_2}{q_2} - \frac{a}{b} \right|.$$

In particular, this implies

$$C\left(\frac{p_2}{q_2}\right) = \frac{q_1 q_3}{q_2} > \frac{1}{3}. \quad (25)$$

For a proof of (i) see Section 3.2.3, for a proof of (ii) see Section 4.6.

Examples 3.7. Since $(\frac{0}{1}, \frac{2}{5}, \frac{1}{2})$ and $(\frac{2}{5}, \frac{12}{29}, \frac{1}{2})$ are centered rational Markov triples,

(i) the best approximants of $\frac{2}{5}$ are $\frac{0}{1}$ and $\frac{1}{2}$, and $C(\frac{2}{5}) = \frac{2}{5}$,

(ii) the best approximants of $\frac{12}{29}$ are $\frac{2}{5}$ and $\frac{1}{2}$, and $C(\frac{12}{29}) = \frac{10}{29}$.

Figure 11 illustrates the geometric interpretation of these examples.

The plane forest of centered rational Markov triples (see Section 2.2 and Figure 3) is constructed in the following lemma. It is used in Section 3.2.3 for the proof Theorem 3.6 (i) and in Section 4.2 to establish the geometric characterization of rational Markov triples.

Lemma 3.8 (Forest of centered rational Markov triples).

(i) If $(\frac{p_1}{q_1}, \frac{p_2}{q_2}, \frac{p_3}{q_3})$ is a rational Markov triple, then so are its children

$$\left(\frac{p_1}{q_1}, \frac{p_3}{q_3}, \frac{p_2}{q_2}\right) \quad \text{and} \quad \left(\frac{p_2}{q_2}, \frac{p_1}{q_1}, \frac{p_3}{q_3}\right) \quad (26)$$

and its parents

$$\left(\frac{p_2'}{q_2'}, \frac{p_1}{q_1}, \frac{p_3}{q_3}\right), \quad \left(\frac{p_1}{q_1}, \frac{p_3}{q_3}, \frac{p_2'}{q_2'} + 3\right) \quad (27)$$

where q_1' , q_2' , and q_3' are defined by (15), and p_1' , p_2' , and p_3' defined by

$$p_1' = \frac{1}{q_1} (p_2 q_2 + p_3 q_3), \quad (28)$$

$$p_2' = p_3 p_1 - \frac{p_1^2 + 1}{q_1} q_3, \quad (29)$$

$$p_3' = \frac{1}{q_3} (p_1 q_1 + p_2 q_2). \quad (30)$$

In particular, $p_k' \in \mathbb{Z}$ for $k \in \{1, 2, 3\}$.

- (ii) A rational Markov triple is a child of each of its parents and a parent of each of its children.
- (iii) Both children of a centered rational Markov triple are centered, and exactly one parent of a non-singular centered rational Markov triple is centered.

Thus, the parent-child relationship induces on the set of non-integer centered rational Markov triples the structure of a plane binary forest, with singular root triples $(n, n + \frac{1}{2}, n + 1)$ as shown in Figure 4 and the generating rule (5).

3.2.1 Proof of Lemma 3.2 (Completion of rational Markov triples)

To see part (i) of Lemma 3.2, first note that q_2 divides $p_2^2 + 1$ because q_2 and q_1 are coprime and

$$q_1^2 (p_2^2 + 1) \stackrel{(16)}{=} (p_1 q_2 + q_3)^2 + q_1^2 \stackrel{(13)}{=} q_2 (p_1^2 q_2 + 2 p_1 q_3 + 3 q_1 q_3 - q_2).$$

A straightforward calculation yields equation (17):

$$p_3 q_2 - p_2 q_3 \stackrel{(21)}{=} p_2 (p_2 q_1 - p_1 q_2) + q_1 - p_2 q_3 \stackrel{(16)}{=} q_1$$

Statement (ii) can be proved in the same way.

For the integrality statement of (iii), consider the identity

$$q_1 (p_1 q_1 + p_3 q_3) \stackrel{(19)}{=} p_1 (q_1^2 + q_3^2) + q_2' q_3 \stackrel{(15)}{=} q_2' (p_1 q_2 + q_3).$$

So q_2' divides $(p_1 q_1 + p_3 q_3)$ because q_1 and q_2' are coprime as elements of the Markov triple (q_1, q_2', q_3) .

To verify equations (16) and (17), use the equivalent forms (18): With

$$\frac{p_2}{q_2} \stackrel{(23)}{=} \frac{p_1 q_1 + p_3 q_3}{q_2 q_2'} \stackrel{(15)}{=} \frac{p_1 q_1 + p_3 q_3}{q_1^2 + q_3^2}$$

we obtain

$$\frac{p_2}{q_2} - \frac{p_1}{q_1} \stackrel{(23)}{=} \frac{(p_3 q_1 - p_1 q_3) q_3}{(q_1^2 + q_3^2) q_1} \stackrel{(19)}{=} \frac{q_2' q_3}{(q_1^2 + q_3^2) q_1} \stackrel{(15)}{=} \frac{q_3}{q_1 q_2},$$

proving (16). An analogous calculation proves (17).

Finally, since it has been established that $(\frac{p_1}{q_1}, \frac{p_2}{q_2}, \frac{p_3}{q_3})$ is a rational Markov triple, the uniqueness of the completion follows from equations (18). \square

3.2.2 Proof of Lemma 3.8 (Forest of centered rational Markov triples)

Parts (i) and (ii) of Lemma 3.8 can be proved by applying the Completion-Lemma 3.2 appropriately. For example, to see that the first child is a rational Markov triple, let $\frac{\tilde{p}_1}{\tilde{q}_1} = \frac{p_1}{q_1}$ and $\frac{\tilde{p}_3}{\tilde{q}_3} = \frac{p_2}{q_2}$. Then

$$\tilde{p}_3 \tilde{q}_1 - \tilde{p}_1 \tilde{q}_3 = q_3 =: \tilde{q}_2',$$

and Lemma 3.2 (iii) says that

$$\left(\frac{\tilde{p}_1}{\tilde{q}_1}, \frac{\tilde{p}_2}{\tilde{q}_2}, \frac{\tilde{p}_3}{\tilde{q}_3} \right) = \left(\frac{p_1}{q_1}, \frac{p_3'}{q_3'}, \frac{p_2}{q_2} \right)$$

is a rational Markov triple.

Statement (iii) follows from the same properties of Markov triples and their neighbors that produce the tree of Markov numbers [6]: If $q_2 \geq \max\{q_1, q_3\}$, then $q'_1 > q_2$ and $q'_3 > q_2$, so both children of a centered rational Markov triple are centered. If $q_2 > \max\{q_1, q_3\} > 1$, then $\min\{q_1, q_3\} \leq q'_2 < \max\{q_1, q_3\}$, so exactly one parent of a non-singular centered rational Markov triple is centered. Finally, consider a singular but non-integer centered rational Markov triple. It is of the form $(n, n + \frac{1}{2}, n + 1)$, and its parents are the integer triples $(n - 1, n, n + 1)$ and $(n, n + 1, n + 2)$, which are both centered. Therefore, starting with any non-integer centered rational Markov triple and traversing up the parental line along centered triples, one will eventually reach a pair of adjacent integer triples. The generating rule (5) is equivalent to the equations for children. \square

3.2.3 Proof of Theorem 3.6 (i). Every Markov fraction is the middle element of a unique centered triple

By definition, every Markov fraction $\frac{p}{q}$ is contained in some rational Markov triple. If q is not the largest denominator in that triple, iteratively replace the triple with the parent or child in which the fraction with largest denominator is removed until q is the largest denominator. If $\frac{p}{q}$ is not the middle element in this triple then it is the middle element in one of the adjacent triples (20). This shows that there exists a centered rational Markov triple m with $\frac{p}{q}$ in the middle.

To see that m is the unique centered rational Markov triple with $\frac{p}{q}$ in the middle, consider first the tree of centered rational Markov triples that contains m . All descendants of m have a larger denominator in the middle, and all ancestors have a smaller denominator in the middle. So no other centered triple in the same tree has $\frac{p}{q}$ in the middle. But each tree in the forest of centered rational Markov triples contains only Markov fractions in a unique integer interval $[n, n + 1]$. So if a Markov fraction is contained in two centered rational Markov triples of different trees, then it is an integer, and it is the last element in one triple and the first element in the other. This shows that no two centered rational Markov triples have the same middle element. \square

3.3 Companions of Markov fractions

This section deals with the other type of worst approximable rational numbers, the companions of Markov fractions (see Theorems 2.1 and 3.15).

Definition 3.9. The *right companions* and *left companions* of a Markov fraction $\frac{p}{q}$ are the rational numbers $\gamma_k^+(\frac{p}{q})$ and $\gamma_k^-(\frac{p}{q})$ for $k \geq 2$, defined by

$$\gamma_k^\pm\left(\frac{p}{q}\right) = \frac{p}{q} \pm \frac{u_{k-1}}{q u_k}, \quad (31)$$

where (u_k) is the integer sequence determined by the recursion

$$u_0 = 0, \quad u_1 = 1, \quad u_{k+1} = 3q u_k - u_{k-1}. \quad (32)$$

We will often use the following lemma implicitly (e.g., in the statement of Theorem 3.15).

Lemma 3.10. *The common denominator on the right hand side of equation (31) is indeed $q u_k$, so the fraction representation*

$$\gamma_k^\pm\left(\frac{p}{q}\right) = \frac{p u_k \pm u_{k-1}}{q u_k}$$

is reduced.

Proof. See Corollary 4.7. □

Remark 3.11 (Index issues). For $k = 1$, equation (31) says

$$\gamma_1^\pm\left(\frac{p}{q}\right) = \frac{p}{q}, \quad (33)$$

But Definition 3.9 explicitly requires $k \geq 2$, so the Markov fraction $\frac{p}{q}$ is by definition not a companion of itself. Consequently, *the k -th left and right companions* are $\gamma_{k+1}^+\left(\frac{p}{q}\right)$ and $\gamma_{k+1}^-\left(\frac{p}{q}\right)$, respectively. One could fix this notational nuisance either by changing the definition and counting the Markov fractions as their own companions, or by shifting the index in the definition of γ_k^\pm . The first option is bad because Markov fractions and their companions are different both regarding Diophantine approximation (compare Theorems 3.6 and 3.15) and from the geometric point of view (compare Lemmas 4.2 and 4.4). The second option is bad because it would create other nuisances. For example, the symmetries (34) and (35) of the following remark would become more complicated.

Remark 3.12 (Symmetry). The recursion (32) can be used to define u_k and hence γ_k^\pm not only for $k \geq 0$ but for all $k \in \mathbb{Z}$. Then

$$u_{-k} = -u_k \quad (34)$$

and this implies $\gamma_0^\pm\left(\frac{p}{q}\right) = \infty$ and the following symmetry relating γ^+ and γ^- :

$$\gamma_{-k}^+\left(\frac{p}{q}\right) = \gamma_k^-\left(\frac{p}{q} + 3\right) \quad (35)$$

The following properties of the sequence $(u_k)_{k \in \mathbb{Z}}$ are easily verified by induction.

Lemma 3.13 (Properties of u_k). *For any Markov number q , the sequence $(u_k)_{k \in \mathbb{Z}}$ defined by (32) is*

- (i) *strictly increasing and*
- (ii) *satisfies the equation*

$$u_{k+1}^2 - 3q u_{k+1} u_k + u_k^2 = 1 \quad (36)$$

for all $k \in \mathbb{Z}$.

Remark 3.14 (Fibonacci and Pell numbers). (i) For $q = 1$,

$$u_k = F_{2k} \quad \text{and so} \quad \gamma_k^\pm(p) = p + \frac{F_{2k-2}}{F_{2k}},$$

where (F_k) is the sequence of Fibonacci numbers,

$$F_0 = 0, \quad F_1 = 1, \quad F_{k+1} = F_k + F_{k-1}.$$

(ii) For $q = 2$ and odd p ,

$$2u_k = P_{2k} \quad \text{and so} \quad \gamma_k^\pm\left(\frac{p}{2}\right) = \frac{p}{2} \pm \frac{P_{2k-2}}{2P_{2k}},$$

where (P_k) is the sequence of Pell numbers,

$$P_0 = 0, \quad P_1 = 1, \quad P_{k+1} = 2P_k + P_{k-1}.$$

Theorem 3.15 (Best approximants of companions). *The best approximants of a companion $\gamma_k^\pm(\frac{p}{q})$, $k \geq 2$, are precisely $\frac{p}{q}$ and $\gamma_{k-1}^\pm(\frac{p}{q})$, i.e.,*

$$C\left(\gamma_k^\pm\left(\frac{p}{q}\right)\right) = q^2 \left| \gamma_k^\pm\left(\frac{p}{q}\right) - \frac{p}{q} \right| = (qu_{k-1})^2 \left| \gamma_k^\pm\left(\frac{p}{q}\right) - \gamma_{k-1}^\pm\left(\frac{p}{q}\right) \right| \quad (37)$$

and

$$C\left(\gamma_k^\pm\left(\frac{p}{q}\right)\right) < b^2 \left| \gamma_k^\pm\left(\frac{p}{q}\right) - \frac{a}{b} \right|$$

for every rational number $\frac{a}{b}$ except $\frac{p}{q}$, $\gamma_{k-1}^\pm(\frac{p}{q})$, and $\gamma_k^\pm(\frac{p}{q})$. Moreover,

$$C\left(\gamma_k^\pm\left(\frac{p}{q}\right)\right) = q \frac{u_{k-1}}{u_k} \geq \frac{1}{3}, \quad (38)$$

where equality holds if and only if $k = 2$, i.e., for first companions.

The first companions $\gamma_2^\pm(\frac{p}{q})$ with approximation constant $C = \frac{1}{3}$ are therefore the best of the worst approximable rational numbers. They are also distinguished by the property that the approximation constant is attained for one unique best approximant, $\frac{p}{q} = \gamma_1^\pm(\frac{p}{q})$, instead of two.

Examples 3.16. (i) The first right and left companions of the Markov fraction $\frac{1}{2}$ are $\gamma_2^+(\frac{1}{2}) = \frac{7}{12}$ (compare Table 1) and $\gamma_2^-(\frac{1}{2}) = \frac{5}{12}$. They are best approximated by their associated Markov fraction $\frac{1}{2}$ and no other rational number. The approximation constant is $C(\frac{7}{12}) = C(\frac{5}{12}) = \frac{1}{3}$.

(ii) The second right and left companions of $\frac{1}{2}$ are $\gamma_3^+(\frac{1}{2}) = \frac{41}{70}$ (compare Table 1) and $\gamma_3^-(\frac{1}{2}) = \frac{29}{70}$. They are best approximated by exactly two rational numbers: their associated Markov fraction $\frac{1}{2}$ and its first right and left companion, respectively. The approximation number is $C(\frac{41}{70}) = C(\frac{29}{70}) = \frac{12}{35}$.

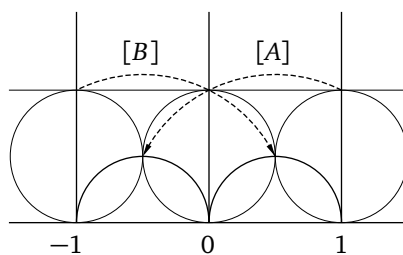


Figure 10: Fundamental domain of the modular torus with gluing transformations

4 The geometric point of view

4.1 The modular torus

Let $G = \langle [A], [B] \rangle \subset PSL_2(\mathbb{Z})$ be the subgroup of orientation preserving hyperbolic isometries generated by

$$[A] = \begin{bmatrix} 1 & -1 \\ -1 & 2 \end{bmatrix} \quad \text{and} \quad [B] = \begin{bmatrix} 1 & 1 \\ 1 & 2 \end{bmatrix}.$$

The *modular torus* is the quotient space $M = H^2/G$ with canonical projection

$$\pi : H^2 \longrightarrow M, \quad \pi(z) = Gz.$$

The ideal quadrilateral with vertices -1 , 0 , 1 , and ∞ is a fundamental domain, from which one obtains the torus M by gluing the pairs of opposite sides via the isometries $[A]$ and $[B]$, respectively (see Figure 10).

The Farey triangulation of the projective plane H^2 projects to the most symmetric ideal triangulation of M , and the Ford circles project to the boundary of the largest embedded cusp neighborhood in M .

4.2 The geometric characterization of rational Markov triples and Markov fractions

Rational Markov triples correspond to the fundamental domains of the modular torus M that are ideal quadrilaterals with one vertex at ∞ . This is illustrated in Figure 10 for the triple $(-1, 0, 1)$, in Figure 11 for the triples $(\frac{0}{1}, \frac{2}{5}, \frac{1}{2})$ and $(\frac{2}{5}, \frac{12}{29}, \frac{1}{2})$, and schematically in Figure 12.

Remark 4.1. For the sake of clearer pictures, Figures 12, 14, and 16 do not show the correct geometry of the modular torus M but some other hyperbolic tori with one cusp. As a result, the objects in these figures are more evenly sized and intersect each other less than would be the case in the modular torus.

To put the correspondence between rational Markov triples and fundamental domains more precisely, we formulate the following lemma:

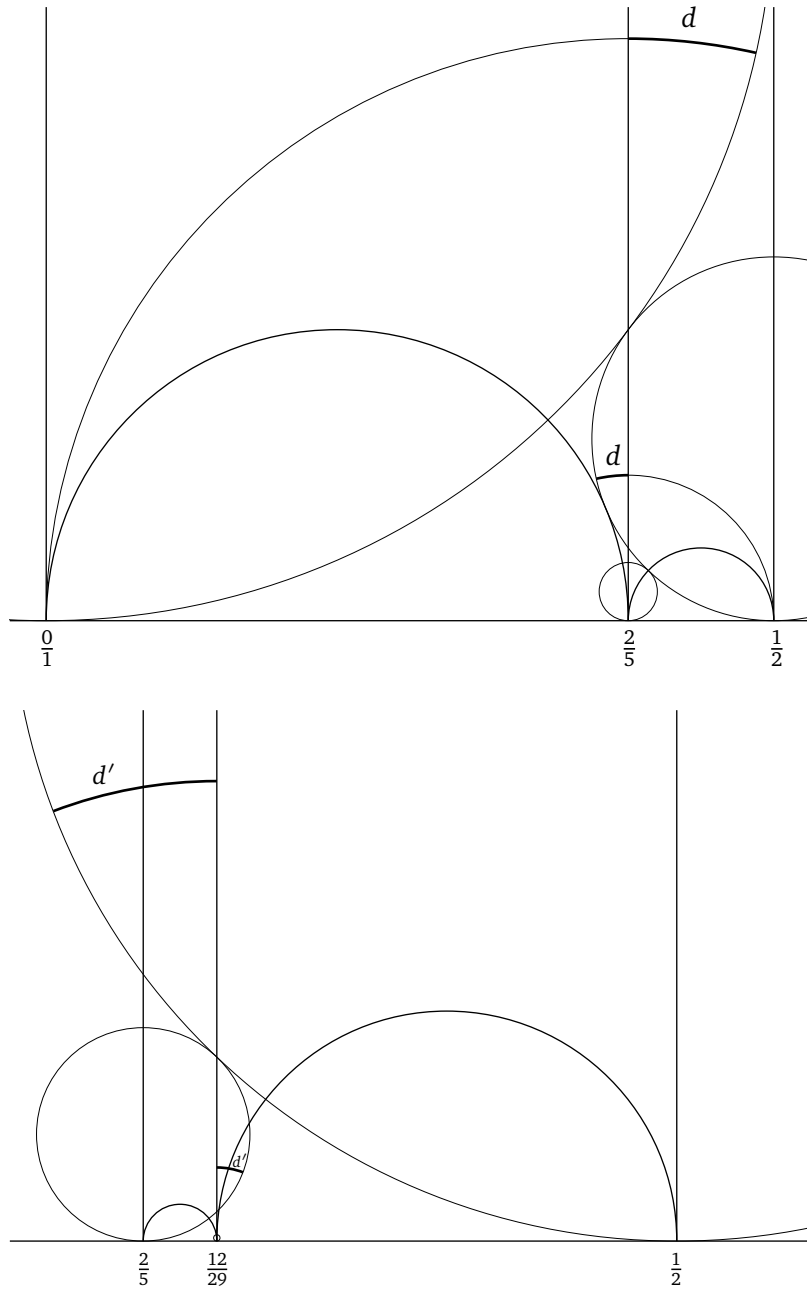


Figure 11: Fundamental domains corresponding to the centered rational Markov triples $(\frac{0}{1}, \frac{2}{5}, \frac{1}{2})$ and $(\frac{2}{5}, \frac{12}{29}, \frac{1}{2})$ of Example 3.7. The approximation constants of $\frac{2}{5}$ and $\frac{12}{29}$ are $e^{\frac{1}{2}d} = C(\frac{2}{5}) = \frac{2}{5}$ and $e^{\frac{1}{2}d'} = C(\frac{12}{29}) = \frac{10}{29}$, respectively (see Lemma 2.8 and Corollary 2.9). The signed distances d and d' are negative because the vertical geodesics at $\frac{2}{5}$ and $\frac{12}{29}$ intersect the Ford circles at the best approximants.

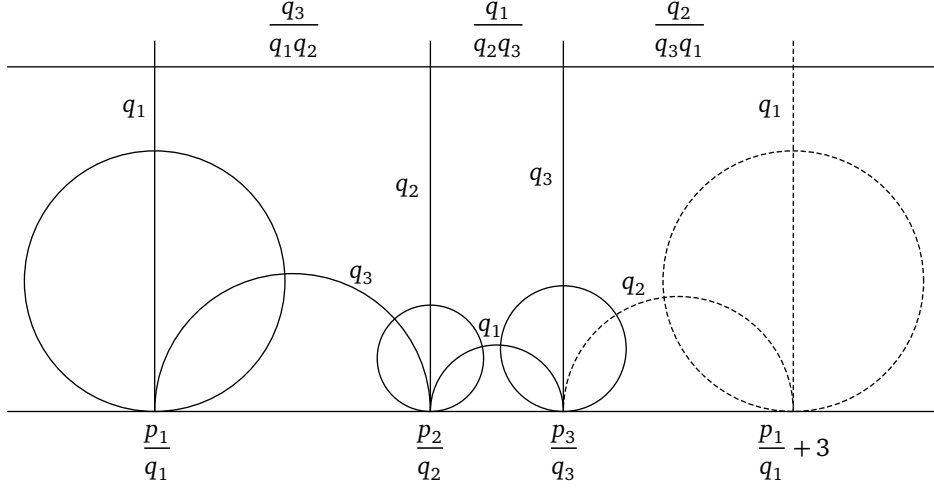


Figure 12: If $(\frac{p_1}{q_1}, \frac{p_2}{q_2}, \frac{p_3}{q_3})$ is a rational Markov triple, then the ideal quadrilateral with vertices $\frac{p_1}{q_1}, \frac{p_2}{q_2}, \frac{p_3}{q_3}$, and ∞ is a fundamental domain of the modular torus. *Dashed*: If we cut along the diagonal q_2 and glue the left ideal triangle $\frac{p_1}{q_1}, \frac{p_2}{q_2}, \infty$ back to the right ideal triangle $\frac{p_2}{q_2}, \frac{p_3}{q_3}, \infty$, but along edge q_3 , we obtain another fundamental domain, which corresponds to the rational Markov triple $(\frac{p_2}{q_2}, \frac{p_3}{q_3}, \frac{p_1}{q_1} + 3)$ (compare equation (20)).

Lemma 4.2 (Geometric characterization of rational Markov triples). *The following statements for real numbers $x_1 < x_2 < x_3$ are equivalent:*

- (i) (x_1, x_2, x_3) is a rational Markov triple.
- (ii) The ideal quadrilateral with vertices x_1, x_2, x_3, ∞ is a fundamental domain of the modular torus M .
- (iii) The ideal triangles with vertices x_1, x_2, ∞ and x_2, x_3, ∞ , respectively, project to the two triangles of some ideal triangulation of the modular torus M .

(For a proof, see Section 4.3.)

Since every simple geodesic with both ends in the cusp is an edge of some ideal triangulation of the modular torus M , we get the following characterization of Markov fractions:

Corollary 4.3 (Geometric characterization of Markov fractions). *For a real number $x \in \mathbb{R}$, the following statements are equivalent:*

- (i) x is a Markov fraction.
- (ii) The vertical geodesic g_x joining x and ∞ in H^2 projects to a simple geodesic $\pi(g_x)$ in the modular torus M with both ends in the cusp.

4.3 Proof of Lemma 4.2 (Geometric characterization of rational Markov triples)

The equivalence of statements (ii) and (iii) of the lemma is obvious. It remains to show that (i) and (iii) are equivalent.

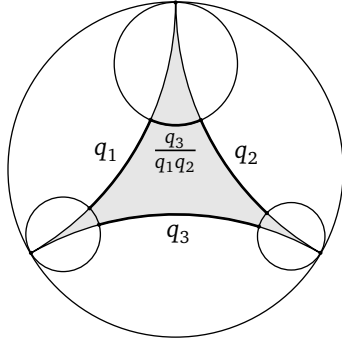


Figure 13: Ideal triangle decorated with horocycles. Relation between edge weights q_k and horocyclic arcs

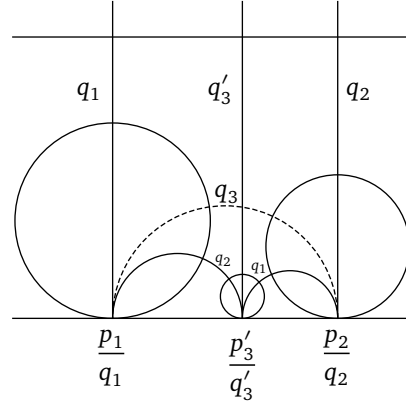


Figure 14: Fundamental domain consisting of ideal triangles $\frac{p_1}{q_1}, \frac{p'_3}{q'_3}, \infty$ and $\frac{p'_3}{q'_3}, \frac{p_2}{q_2}, \infty$

(iii)⇒(i). Assuming (iii) implies that the vertices $x_k \in \mathbb{R}$ are rational,

$$x_k = \frac{p_k}{q_k} \in \mathbb{Q},$$

because they project to the ideal point of the modular torus.

The denominators q_k are equal to the weights of the edges of the triangulation [32, Ch. 11] (see Figure 12). Indeed, the euclidean diameter of the Ford circle at $\frac{p_k}{q_k}$ is q_k^{-2} , so the distance to the horocycle $\{\text{Im}z = 1\}$ is $d_k = 2 \log q_k$, and the weight is $q_k = e^{d_k/2}$.

By Penner's geometric interpretation of Markov's equation [25, 26], the denominators form a Markov triple (q_1, q_2, q_3) . Finally, the relation between the edge weights and the horocyclic arcs of a decorated ideal triangle (see Figure 13) implies equations (18). Therefore, $(x_1, x_2, x_3) = \left(\frac{p_1}{q_1}, \frac{p_2}{q_2}, \frac{p_3}{q_3}\right)$ is a rational Markov triple.

(i)⇒(iii). The implication is true for any integer rational Markov triple, i.e., if $(x_1, x_2, x_3) = (n-1, n, n+1)$ for some $n \in \mathbb{Z}$. We will show: If the implication is true for a rational Markov triple $\left(\frac{p_1}{q_1}, \frac{p_2}{q_2}, \frac{p_3}{q_3}\right)$, then it also holds for the adjacent triples (20) and the children (26). Since every centered rational Markov triple is a descendant of an integer triple, and every non-centered rational Markov triple is adjacent to a centered one, this proves the implication (i)⇒(iii) for all rational Markov triples.

So let $\left(\frac{p_1}{q_1}, \frac{p_2}{q_2}, \frac{p_3}{q_3}\right)$ be a rational Markov triple for which the implication (i)⇒(iii) holds. To see that the same is true for the adjacent triples (20), note that $z \mapsto z+6$ is a deck transformation of the modular torus, and $z \mapsto z+3$ is a lift of the elliptic involution.

It remains to show that the implication (i) \Rightarrow (iii) also holds for the children (26). We will present the argument for the left child $(\frac{p_1}{q_1}, \frac{p'_3}{q'_3}, \frac{p_2}{q_2})$, see Figure 14. The argument for the right child is analogous.

First we choose a matrix $S \in SL_2(\mathbb{R})$ that satisfies

$$S \begin{pmatrix} p_1 \\ q_1 \end{pmatrix} = \pm \begin{pmatrix} p_2 \\ q_2 \end{pmatrix} \quad \text{and} \quad S \begin{pmatrix} p_2 \\ q_2 \end{pmatrix} = \pm \begin{pmatrix} p_1 \\ q_1 \end{pmatrix},$$

which determines S up to sign. Let us choose

$$\begin{aligned} S &= \begin{pmatrix} p_2 & p_1 \\ q_2 & q_1 \end{pmatrix} \cdot \begin{pmatrix} -p_1 & p_2 \\ -q_1 & q_2 \end{pmatrix}^{-1} \\ &= \frac{1}{p_2q_1 - p_1q_2} \begin{pmatrix} p_1q_1 + p_2q_2 & -p_1^2 - p_2^2 \\ q_1^2 + q_2^2 & -p_1q_1 - p_2q_2 \end{pmatrix}. \end{aligned}$$

Then the hyperbolic isometry $[S] \in PSL_2(\mathbb{R})$ maps the Ford circle $h(p_1, q_1)$ at $\frac{p_1}{q_1}$ to the Ford circle $h(p_2, q_2)$ at $\frac{p_2}{q_2}$ and vice versa (see Section 2.9). This implies that $[S] \in PSL_2(\mathbb{R})$ is a lift of the elliptic involution of the modular torus M , and therefore $S \in SL_2(\mathbb{Z})$.

Since the ideal triangle with vertices $\frac{p_1}{q_1}, \frac{p_2}{q_2}, \infty$ is a lift of one triangle of an ideal triangulation of the modular torus, the ideal triangle with vertices

$$[S] \cdot \frac{p_1}{q_1} = \frac{p_2}{q_2}, \quad [S] \cdot \frac{p_2}{q_2} = \frac{p_1}{q_1}, \quad \text{and} \quad [S] \cdot \infty$$

is a lift of the other triangle of the triangulation. (Here \cdot denotes the isometric action of $PSL_2(\mathbb{R})$ on H^2 .) Applying an edge flip, we obtain a triangulation of the modular torus whose triangles lift to the ideal triangles with vertices

$$\frac{p_1}{q_1}, \quad S \cdot \infty, \quad \infty \quad \text{and} \quad S \cdot \infty, \quad \frac{p_2}{q_2}, \quad \infty,$$

respectively. Finally, using equation (16) and $(q_1^2 + q_2^2)/q_3 = q'_3$, we obtain

$$S \begin{pmatrix} 1 \\ 0 \end{pmatrix} = \begin{pmatrix} p'_3 \\ q'_3 \end{pmatrix}, \quad \text{so} \quad S \cdot \infty = \frac{p'_3}{q'_3}$$

and the implication (i) \Rightarrow (iii) holds for the child $(\frac{p_1}{q_1}, \frac{p'_3}{q'_3}, \frac{p_2}{q_2})$, too. This completes the proof of Lemma 4.2. \square

4.4 The geometric characterization of companions

For a Markov fraction x , Figure 15 schematically illustrates the geometric interpretation of the the first right companion $\gamma_2^+(x)$.

Generally, the vertical geodesic g_x projects to a simple geodesic $\pi(g_x)$ in the Modular torus M with both ends in the cusp (by Corollary 4.3). Then there is a

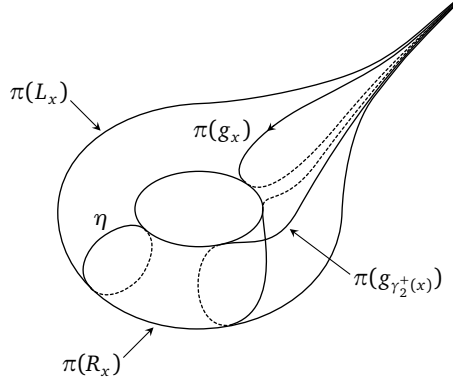


Figure 15: Topological sketch of the modular torus M showing the geodesic $\pi(g_x)$ corresponding to a Markov fraction x , and the simple closed geodesic η that does not intersect it. The geodesic $\pi(g_{\gamma_2^+(x)})$ corresponds to the first right companion $\gamma_2^+(x)$. It is contained in the cylinder $\pi(R_x)$ bounded by $\pi(g_x)$ and η and has one self-intersection.

unique simple closed geodesic η in M that does not intersect $\pi(g_x)$. The geodesics $\pi(g_x)$ and η separate M into two cylinders, which are labeled $\pi(R_x)$ and $\pi(L_x)$ in Figure 15 for reasons that will become clear in the following Section 4.5. Be that as it may, $\pi(R_x)$ is the cylinder to the right of $\pi(g_x)$ if g_x is oriented in the direction from x to ∞ , and $\pi(L_x)$ is the cylinder to the left.

Now let y be a right or left companion of x , i.e., $y = \gamma_k^+(x)$ or $y = \gamma_k^-(x)$ for some $k \geq 2$. Then the vertical geodesic g_y projects to a non-simple geodesic $\pi(g_y)$ in the cylinder $\pi(R_x)$ or $\pi(L_x)$, respectively, with $k - 1$ self-intersections.

Formulating the converse statement is slightly more involved. To understand why, note first of all that the isometry $z \mapsto z + 6$ of H^2 is a deck transformation of M , so the companions of x correspond to the same vertical geodesics in M as the companions of $x + 6n$ for any $n \in \mathbb{Z}$. Secondly, the isometry $z \mapsto z + 3$ of H^2 projects to the hyperelliptic involution of M , which reverses the orientations of $\pi(g_x)$ and η . As a consequence, the cylinder $\pi(R_x)$ contains not only the projected vertical geodesics for the right companions $\gamma_k^+(x)$, but also those for $\gamma_k^-(x - 3)$, the left companions of $x - 3$ (compare Remark 3.12).

Altogether, the following lemma characterizes the right and left companions of a Markov fraction geometrically:

Lemma 4.4 (Geometric characterization of companions). *Let x be a Markov fraction, so that $\pi(g_x)$ is a simple geodesic in the modular torus M with both ends in the cusp. Let η be the unique simple closed geodesic in M that does not intersect $\pi(g_x)$. Then for a number $y \in \mathbb{R}$ and the vertical geodesic g_y , the statements (i^+) and (ii^+) are equivalent, and the statements (i^-) and (ii^-) are equivalent:*

- (i^+) y is a right companion of x , i.e., $y = \gamma_k^+(x)$ for some $k \geq 2$.
- (ii^+) $y \in [x, x + \frac{3}{2}]$ and $\pi(g_y)$ is a geodesic with both ends in the cusp that intersects neither $\pi(g_x)$ nor η .

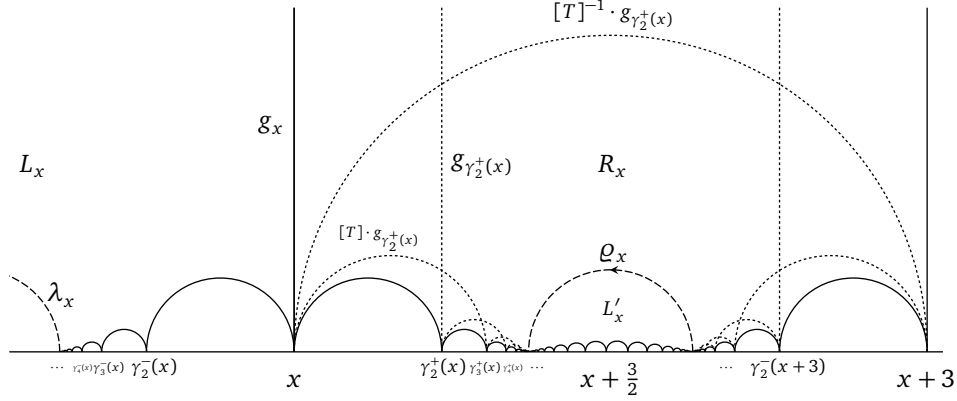


Figure 16: The right companions $\gamma_2^+(x), \dots$ are ideal vertices of region R_x between x and $x + \frac{3}{2}$. The left companions $\gamma_2^-(x), \dots$ are ideal vertices of the region L_x between $x - \frac{3}{2}$ and x . The dotted lines are the geodesics $[T]^k \cdot g_{\gamma_2^+(x)}$.

- (i⁻) y is a left companion of x , i.e., $y = \gamma_k^-(x)$ for some $k \geq 2$.
- (ii⁻) $y \in [x - \frac{3}{2}, x]$ and $\pi(g_y)$ is a geodesic with both ends in the cusp that intersects neither $\pi(g_x)$ nor η .

The geodesics $\pi(g_{\gamma_k^+(x)})$ and $\pi(g_{\gamma_k^-(x)})$ have $k - 1$ self-intersections.

4.5 Proof of Lemma 4.4 (Geometric characterization of companions)

The geodesics in the G -orbit $G \cdot g_x$ of the vertical geodesic g_x together with $\pi^{-1}(\eta)$, the G -orbit of lifts of the closed geodesic η , separate the hyperbolic plane H^2 into simply connected domains. Each one of these domains covers one of the two cylinders into which $\pi(g_x)$ and η separate M . Of these domains, let R_x and L_x be the ones to the right and to the left of g_x , respectively, when g_x is oriented in the direction from x to ∞ (see Figure 16). In short, R_x and L_x are the domains to the left and right of g_x such that the restrictions $\pi|_{R_x}$ and $\pi|_{L_x}$ are universal covers of the two cylinders in M .

The geometric characterization of companions follows in a straightforward manner from an explicit analytic description of the domains R_x and L_x . We will perform the calculations only for R_x and the right companions $\gamma_k^+(x)$. The domain L_x and the left companions $\gamma_k^-(x)$ can be treated analogously. Alternatively, one may use the fact that $z \mapsto z + 3$ projects to the elliptic involution to see that $L_x = R_x - 3$ (compare Remark 3.12).

Let the Markov fraction be $x = \frac{p}{q}$. Then the group of deck transformations of the universal cover $R_x \rightarrow \pi(R_x)$ is generated by the hyperbolic isometry

$$[T] \in G \subset \text{PSL}_2(\mathbb{Z})$$

that maps the Ford circle $h(1, 0)$ at ∞ to the Ford circle $h(p, q)$ at x , and the Ford

circle $h(p+3q, q)$ at $x+3$ to the Ford circle $h(1, 0)$ at ∞ . To see this, contemplate Figure 12 with $\frac{p_1}{q_1} = \frac{p}{q}$.

This determines the matrix $T \in SL_2(\mathbb{Z})$ up to sign. Choosing

$$T \begin{pmatrix} 1 & p+3q \\ 0 & q \end{pmatrix} = \begin{pmatrix} -p & 1 \\ -q & 0 \end{pmatrix},$$

which works because

$$\det \begin{pmatrix} 1 & p+3q \\ 0 & q \end{pmatrix} = q = \det \begin{pmatrix} -p & 1 \\ -q & 0 \end{pmatrix}$$

we obtain

$$T = \begin{pmatrix} -p & 3p + \frac{p^2+1}{q} \\ -q & 3q + p \end{pmatrix} \in SL_2(\mathbb{Z}). \quad (39)$$

Remark 4.5. In particular, this implies $\frac{p^2+1}{q} \in \mathbb{Z}$, which provides a geometric interpretation of the number theoretic Corollary 3.3. More directly, such a geometric interpretation can be obtained by considering the orientation preserving hyperbolic isometry $[S_{p,q}] \in PSL_2(\mathbb{R})$ that interchanges the horocycles $h(p, q)$ and $h(1, 0)$. This determines

$$S_{p,q} = \begin{pmatrix} -p & \frac{p^2+1}{q} \\ -q & p \end{pmatrix} \in SL_2(\mathbb{R})$$

up to sign. Since $[S_{p,q}]$ projects to the hyperelliptic involution on M , we have $S_{p,q} \in SL_2(\mathbb{Z})$. (The map $[T]$ is the composition of $[S_{p,q}]$ followed by $z \mapsto z+3$.)

Let ϱ_x be the axis of the hyperbolic translation $[T]$. It projects to the closed geodesic η in M , i.e., $\pi(\varrho_x) = \eta$. The geodesic ϱ_x connects the repelling and attracting fixed points of $[T]$, let us call them ξ_- and ξ_+ . By a straightforward calculation we obtain

$$\xi_{\pm} = x + \frac{3}{2} \mp \sqrt{\frac{9}{4} - \frac{1}{q^2}}. \quad (40)$$

Remark 4.6. Since $\text{trace}(T) = 3q$, the eigenvalues of T are $\frac{1}{2}(3q \pm \sqrt{9q^2 - 4})$. This also shows the well-known formulas for the lengths of closed geodesics in the modular torus,

$$2 \cosh\left(\frac{\text{length}(\eta)}{2}\right) = 3q, \quad 2 \exp\left(\frac{\text{length}(\eta)}{2}\right) = 3q + \sqrt{9q^2 - 4},$$

but we will not need them.

The region R_x is bounded by the geodesic ϱ_x together with the infinite ideal polygon with sides $[T]^k \cdot g_x$ for $k \in \mathbb{Z}$, which connect the ideal vertices $[T]^k \cdot \infty$. The endpoints ξ_{\pm} of ϱ_x are the irrational limit points of the rational bi-infinite sequence of ideal vertices:

$$[T]^k \cdot \infty \longrightarrow \xi_{\pm} \quad \text{as } k \longrightarrow \pm\infty. \quad (41)$$

Now the equivalence of the statements (i⁺) and (ii⁺) follows from the fact that

$$[T]^k \cdot \infty = \gamma_k^+(x) \quad (42)$$

(with $\gamma_k^+(x)$ defined by equation (31)). To see this, let $(r_k)_{k \in \mathbb{Z}}$ and $(s_k)_{k \in \mathbb{Z}}$ be defined by

$$\begin{pmatrix} r_k \\ s_k \end{pmatrix} = T^k \begin{pmatrix} -1 \\ 0 \end{pmatrix}, \quad (43)$$

so that

$$[T]^k \cdot \infty = \frac{r_k}{s_k}.$$

Then it suffices to show that

$$\begin{pmatrix} r_k \\ s_k \end{pmatrix} = \begin{pmatrix} p u_k + u_{k-1} \\ q u_k \end{pmatrix} \quad (44)$$

for the sequence $(u_k)_{k \in \mathbb{Z}}$ defined by (32).

First note that q divides s_k for all $k \in \mathbb{Z}$. (This is easy to see by induction in both directions starting from $s_0 = 0$.) Hence we can *define* integer sequences $(t_k)_{k \in \mathbb{Z}}$ and $(u_k)_{k \in \mathbb{Z}}$ by

$$u_k = \frac{s_k}{q} \quad \text{and} \quad t_k = r_k - p u_k.$$

We have to show that $(u_k)_{k \in \mathbb{Z}}$ solves the recursion (32). The initial conditions are easily verified. Using the relation

$$\begin{pmatrix} r_k \\ s_k \end{pmatrix} = \underbrace{\begin{pmatrix} 1 & p \\ 0 & q \end{pmatrix}}_{=: U} \begin{pmatrix} t_k \\ u_k \end{pmatrix},$$

and $\begin{pmatrix} r_{k+1} \\ s_{k+1} \end{pmatrix} = T \begin{pmatrix} r_k \\ s_k \end{pmatrix}$ we obtain the first order recursion formula

$$\begin{pmatrix} t_{k+1} \\ u_{k+1} \end{pmatrix} = \underbrace{\begin{pmatrix} 0 & 1 \\ -1 & 3q \end{pmatrix}}_{U^{-1} T U} \begin{pmatrix} t_k \\ u_k \end{pmatrix}.$$

Eliminate (t_k) using $t_k = u_{k-1}$ to obtain the second-order recursion (32) for $(u_k)_{k \in \mathbb{Z}}$ and equation (44) for r_k and s_k . This completes the proof of equation (42), showing that (i⁺) and (ii⁺) are equivalent.

Finally, to see that the geodesic $\pi(g_{\gamma_k^+(x)})$ in the cylinder $\pi(R_x) \subset M$ has $k-1$ self-intersections, note that the vertical geodesic $g_{\gamma_k^+(x)}$ in the universal cover R_x intersects the $2(k-1)$ geodesics

$$[T]^\ell \cdot g_{\gamma_k^+(x)} \quad \text{for } \ell \in \{1, \dots, k-1\} \cup \{-(k-1), \dots, -1\}. \quad (45)$$

but the intersection points

$$\zeta_\ell = g_{\gamma_k^+(x)} \cap \left([T]^\ell \cdot g_{\gamma_k^+(x)} \right) \quad (46)$$

project in pairs to the same point in M ,

$$\pi(\zeta_\ell) = \pi(\zeta_{-\ell}), \quad (47)$$

because

$$\zeta_\ell = [T]^\ell \cdot \zeta_{-\ell}. \quad (48)$$

This completes the proof of Lemma 4.4. \square

Because $T \in SL_2(\mathbb{Z})$, equation (43) implies that r_k and s_k are coprime for all $k \in \mathbb{Z}$. So the above proof (together with the analogous argument for the left companions) yields the following corollary:

Corollary 4.7. *For all $k \in \mathbb{Z}$, the integers $p u_k + u_{k-1}$ and $q u_k$ are coprime, and so are the integers $p u_k - u_{k-1}$ and $q u_k$.*

4.6 Proof of Theorem 3.6 (ii) (Best approximants of Markov fractions)

Part (i) of Theorem 3.6 was proved without recourse to geometry in Section 3.2.3. The purpose of this section is to prove part (ii). The argument begins algebraically, but geometry will come into play shortly.

Let

$$m = \left(\frac{p_1}{q_1}, \frac{p_2}{q_2}, \frac{p_3}{q_3} \right)$$

be a centered rational Markov triple. Then we have

$$q_1^2 \cdot \left(\frac{p_2}{q_2} - \frac{p_1}{q_1} \right) \stackrel{(16)}{=} \frac{q_1 q_3}{q_2} \stackrel{(17)}{=} q_3^2 \cdot \left(\frac{p_3}{q_3} - \frac{p_2}{q_2} \right),$$

Moreover,

$$\frac{1}{3} < \frac{q_1 q_3}{q_2} \leq 1$$

from equation (14), together with (24) for the upper bound. It remains to show that for every rational number $\frac{a}{b} \notin \left\{ \frac{p_1}{q_1}, \frac{p_2}{q_2}, \frac{p_3}{q_3} \right\}$,

$$\frac{q_1 q_3}{q_2} < b^2 \cdot \left| \frac{p_2}{q_2} - \frac{a}{b} \right|. \quad (49)$$

To see this, we will rely on the geometric characterization of Markov fractions (see Sections 4.4 and 4.5) to narrow down the set of potential best approximants so we can check (49) for the remaining candidates.

So let $x = \frac{p}{q}$ be a Markov fraction, and let $x^* = \frac{p^*}{q^*}$ be a best approximant, i.e., suppose

$$C\left(\frac{p}{q}\right) = (q^*)^2 \cdot \left| \frac{p}{q} - \frac{p^*}{q^*} \right|. \quad (50)$$

By Lemma 2.8, this means that the Ford circle $h(p^*, q^*)$ has the smallest signed distance to the vertical geodesic g_x among all Ford circles except $h(p, q)$ and $h(1, 0)$. This leads to the following necessary geometric condition for best approximants:

Lemma 4.8. *If x is Markov fraction and x^* is a best approximant of x , then no geodesic in the G -orbit of g_x separates g_x and x^* .*

(A geodesic g in the hyperbolic plane H^2 separates a subset $A \in H^2$ and an ideal point $p \in \partial H^2$ if A and p are contained in different connected components of $(H^2 \cup \partial H^2) \setminus (g \cup \partial g)$, where ∂g is the set of the two ideal endpoints of g .)

Proof of Lemma 4.8. Suppose $\tau \cdot g_x$ separates g_x and x' for some $x' = \frac{p'}{q'} \in \mathbb{Q}$ and $\tau \in G$. We have to show that x' is not a best approximant of x .

Since the shortest geodesic ray from x' to g_x intersects $\tau(g_x)$ before reaching g_x ,

$$d(g_x, h(p', q')) > d(\tau(g_x), h(p', q')) = d(g_x, \tau^{-1}(h(p', q'))).$$

Since the Ford circle $\tau^{-1}(h(p', q'))$ has a smaller signed distance to g_x than $h(p', q')$, the number $\tau^{-1} \cdot x'$ approximates x better than x' . \square

Lemma 4.8 implies that x^* is a rational ideal boundary point of one of the domains

$$R_x \quad \text{or} \quad L'_x$$

that are bounded by the geodesic ϱ_x and geodesics in the G -orbit of g_x (see Figure 17) or one of the domains

$$L_x = R_x - 3 \quad \text{and} \quad R'_x = L'_x - 3$$

bounded by λ_x and geodesics in the G -orbit of g_x . In other words, L'_x and R'_x are the lifts of the cylinders $\pi(L_x)$ and $\pi(R_x)$ that are adjacent to the geodesics ϱ_x and λ_x , respectively, while L_x and R_x are the lifts adjacent to the geodesic g_x . (Compare also Figure 16 but note that it does not represent the geometry of the modular torus M correctly whereas Figure 17 does, as explained in Remark 4.1.)

We will now consider all these rational ideal boundary points that are candidates for best approximants in turn. First, let us consider the rational ideal boundary points of R_x , which are:

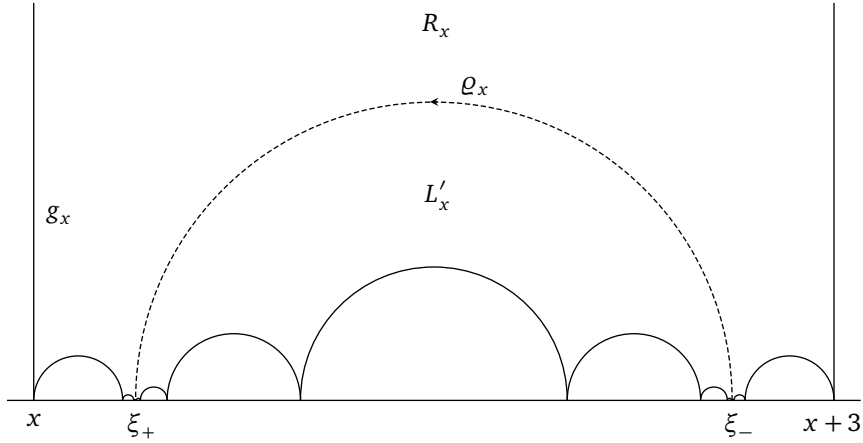


Figure 17: The domains R_x and L'_x bounded by ϱ_x and geodesics in the G -orbit of g_x

- the Markov fraction $x = \frac{p}{q}$ itself, which does not qualify,
- the right companions $\gamma_k^+(x)$, with $k \geq 2$,
- the left companions $\gamma_k^-(x+3)$, also with $k \geq 2$, and
- the Markov fraction $x+3$.

The left companions of $x+3$ are ruled out as best approximants because $\gamma_k^-(x+3)$ has the same denominator as $\gamma_k^+(x)$ but is further away from x .

For a right companion

$$\frac{a}{b} = \gamma_k^+\left(\frac{p}{q}\right),$$

we get using Lemmas 3.10 and 3.13:

$$\begin{aligned} b^2 \cdot \left| \frac{p_2}{q_2} - \frac{a}{b} \right| &= q^2 u_k^2 \left| \frac{p}{q} - \gamma_k^+\left(\frac{p}{q}\right) \right| \\ &\stackrel{(31)}{=} q u_k u_{k-1} \\ &\stackrel{(36)}{=} \frac{1}{3} (u_k^2 + u_{k-1} - 1) \\ &\geq \frac{1}{3} (u_2^2 + u_1 - 1) \\ &\stackrel{(32)}{=} 3q^2 \geq 3 \end{aligned}$$

This means that a right companion $\gamma_k^+(\frac{p}{q})$ approximates the Markov fraction $\frac{p}{q}$ worse than the Markov fractions $\frac{p_1}{q_1}$ and $\frac{p_3}{q_3}$ of the centered rational Markov triple $(\frac{p_1}{q_1}, \frac{p_2}{q_2}, \frac{p_3}{q_3})$ with $\frac{p_2}{q_2} = \frac{p}{q}$.

One ideal boundary point of R_x is left to check: The Markov fraction $x+3$, for which we get $1^2|x-(x+3)|=3$.

Thus we conclude that the ideal boundary points of R_x are not best approximants of x . Similarly, the ideal boundary points of L_x are not best approximants of x .

Remark 4.9. Note that the first companion $\gamma_2^+(x)$ and the Markov fraction $x + 3$ approximate the Markov fraction x exactly equally badly. In general, the $(k-1)$ st right companion $\gamma_k^+(x)$ and the $(k-2)$ nd left companion $\gamma_{k-1}(x+3)$ approximate x with the same approximation quality. This due to a geometric symmetry.

Now let y be a rational ideal boundary point of L'_x . Then the vertical geodesic g_y projects to a simple geodesic $\pi(g_y)$ in M with both ends in the cusp. Furthermore, $\pi(g_y)$ does not intersect of the geodesic $\pi(g_x)$. (To see this, note that g_y does not intersect any of the geodesics $[T]^k \cdot g_y$ for $k \in \mathbb{Z} \setminus \{0\}$, nor any geodesics in the G -orbit of g_x .)

This implies, first, that y is also Markov fraction. Moreover, since $\pi(g_x)$ and $\pi(g_y)$ do not intersect, there are exactly two ideal triangulations of M containing $\pi(g_x)$ and $\pi(g_y)$ as edges. Since $x < y < x + 3$, we can deduce that there is a unique rational Markov triple

$$m' = \left(\frac{p'_1}{q'_1}, \frac{p_2}{q_2}, \frac{p'_3}{q'_3} \right) \quad \text{with} \quad x = \frac{p_2}{q_2}, \quad y = \frac{p'_3}{q'_3}.$$

Conversely, if m' is a rational Markov triple with $x = \frac{p_2}{q_2}$, then $\frac{p'_3}{q'_3}$ is an ideal boundary point of L'_x .

For the ideal boundary point y of L'_x , we get the approximation quality

$$(q'_3)^2 \cdot \left| \frac{p_2}{q_2} - \frac{p'_3}{q'_3} \right| = \frac{q'_3 q'_1}{q_2},$$

and if m' is not the unique centered rational Markov triple m , then

$$\frac{q'_3 q'_1}{q_2} > \frac{q_3 q_1}{q_2}.$$

This shows that among all ideal boundary points of L'_x , the third element $\frac{p'_3}{q'_3}$ of the centered rational Markov triple m with $x = \frac{p_2}{q_2}$ approximates x best, and all other ideal boundary points of L'_x are worse.

In the same way, one sees that among all ideal boundary points of R'_x , the first element $\frac{p_1}{q_1}$ of the centered rational Markov triple m with $x = \frac{p_2}{q_2}$ approximates x best, and all other ideal boundary points of R'_x are worse.

This completes the proof of Theorem 3.6 (ii). \square

Remark 4.10. While many constructions and arguments in this paper generalize to arbitrary hyperbolic tori with one cusp, Theorem 3.6 (ii) really depends on the geometry of the modular torus M . For example, in the torus shown in Figure 16, the horocycles at $\gamma_2^\pm(x)$ are closer to g_x than the horocycles at the ideal boundary points of L'_x and R'_x .

4.7 Proof of Theorem 3.15 (Best approximants of companions)

From the definition (31), we get immediately

$$q^2 \left| \gamma_k^\pm \left(\frac{p}{q} \right) - \frac{p}{q} \right| = q \frac{u_{k-1}}{u_k}.$$

To see that also

$$(q u_{k-1})^2 \left| \gamma_k^\pm \left(\frac{p}{q} \right) - \gamma_{k-1}^\pm \left(\frac{p}{q} \right) \right| = q \frac{u_{k-1}}{u_k},$$

note that

$$\left| \gamma_k^\pm \left(\frac{p}{q} \right) - \gamma_{k-1}^\pm \left(\frac{p}{q} \right) \right| = \frac{1}{q u_k u_{k-1}} \quad (51)$$

because

$$\frac{u_{k-1}}{q u_k} - \frac{u_{k-2}}{q u_{k-1}} = \frac{1}{q u_k u_{k-1}} (u_{k-1}^2 - u_k u_{k-2})$$

and

$$\begin{aligned} u_{k-1}^2 - u_k u_{k-2} &\stackrel{(32)}{=} u_{k-1}^2 - (3q u_{k-1} - u_{k-2}) u_{k-2} \\ &= u_{k-1}^2 - 3q u_{k-1} u_{k-2} + u_{k-2}^2 \\ &\stackrel{(36)}{=} 1. \end{aligned}$$

This shows the right equality in (37).

Remark 4.11. Alternatively, we could avoid these calculations here and infer from a geometric symmetry that $\frac{p}{q}$ and $\gamma_{k-1}^\pm \left(\frac{p}{q} \right)$ both approximate $\gamma_k^\pm \left(\frac{p}{q} \right)$ with the same quality. But we will need equation (51) anyway for the proof of the classification Theorem 2.1 (see Section 4.9).

To see the inequality in (38), note that

$$q u_{k-1} \stackrel{(32)}{=} \frac{1}{3} (u_k + u_{k-2}).$$

So for $k \geq 2$,

$$q \frac{u_{k-1}}{u_k} = \frac{1}{3} \left(1 + \frac{u_{k-2}}{u_k} \right) \geq \frac{1}{3},$$

with equality only for $k = 0$.

It remains to show that

$$q \frac{u_{k-1}}{u_k} < b^2 \left| \gamma_k^\pm \left(\frac{p}{q} \right) - \frac{a}{b} \right| \quad (52)$$

for every rational number $\frac{a}{b}$, except $\frac{p}{q}$, $\gamma_{k-1}^\pm \left(\frac{p}{q} \right)$, and $\gamma_k^\pm \left(\frac{p}{q} \right)$. The general strategy is the same as in the previous section. We will use Lemma 4.14 to eliminate all but a manageable subset of candidates $\frac{a}{b}$ that we have to check. However, instead of G -orbits as in Lemma 4.8, we will consider orbits with respect to a larger group \widehat{G} , of which G is a subgroup of index 2:

Definition 4.12. Let $\widehat{G} \subset PSL_2(\mathbb{Z})$ be the group generated by the group G of deck transformations of M and any lift of the elliptic involution, e.g., $z \mapsto z + 3$.

Remark 4.13. In the previous section, it was sufficient to consider the G -orbits of g_x , because the elliptic involution only reverses the orientation of simple geodesics in M with both ends in the cups. Hence, the G -orbit and the \widehat{G} -orbit of g_x are equal if we disregard the orientation of geodesics.

Lemma 4.14. *If y is a companion of a Markov fraction and y^* is a best approximant of y , then no geodesic in the \widehat{G} -orbit of g_y separates g_y and y^* .*

Lemma 4.14 can be proved in the same way as the analogous Lemma 4.8 for Markov fractions. Next, we will use it to prove a second geometric lemma:

Lemma 4.15. *If y is a companion of a Markov fraction x , and y^* is a best approximant of y , then no geodesic in the G -orbit of g_x separates g_y and y^* .*

Proof. Let us assume that y is a right companion of x , i.e.,

$$y = \gamma_k^+(x), \quad k \geq 2. \quad (53)$$

The argument for left companions is analogous. The proof has two parts.

Part 1. We will first prove the following statement:

For all real numbers $y' < x$ there is a geodesic in the \widehat{G} -orbit of g_y that separates g_x and y' .

To this end, we consider two cases separately:

- $y' \in (-\infty, y - 3)$. Let $\tau(z) = z - 3$. Then $\tau \in \widehat{G}$, and because $y - 3 < x$, the vertical geodesic $\tau \cdot g_y$ separates g_x and y' .
- $y' \in (\gamma_{k-1}^+(x) - 3, x)$. With $[T] \in G$ as in Section 4.5 and τ as above we have

$$[T]^{-1} \cdot y = \gamma_{k-1}^+(x) \quad \text{and} \quad [T]^{-1} \cdot \infty = x + 3.$$

The geodesic $\tau \circ [T]^{-1} \cdot g_y$ therefore has ideal endpoints $\gamma_{k-1}^+(x) - 3$ and x . So it separates g_y and y' .

Since $\gamma_{k-1}^+(x) < y$, the two intervals cover $(-\infty, x)$, and hence we have shown the statement for all $y' < x$.

Part 2. Now to prove the lemma, suppose there is a $\sigma \in G$ such that $\sigma \cdot g_x$ separates g_y and y' . We have to show that y' is not a best approximant of y .

To see this, let $\hat{\sigma} \in \widehat{G}$ be the element with

$$\hat{\sigma} \cdot g_x = \sigma \cdot g_x \quad \text{and} \quad y' \in \hat{\sigma} \cdot \mathbb{R}_{<x}.$$

(Either $\hat{\sigma} = \sigma$, or $\sigma^{-1}\hat{\sigma}$ is the lift of the elliptic involution on M that maps the simple geodesic g_x with both ends in the cusp to itself, but reversing its

orientation.) Then $\hat{\sigma}^{-1} \cdot y' < x$, so by (1) there is a geodesic $g_1 \in \widehat{G} \cdot g_y$ that separates g_x and $\hat{\sigma}^{-1} \cdot y'$. Hence $\hat{\sigma} \cdot g_1$ separates $\hat{\sigma} \cdot g_x$ and y' . Since $\hat{\sigma} \cdot g_x$ separates g_y and y' by assumption, the geodesic $\hat{\sigma} \cdot g_1$ separates g_y and y' . By Lemma 4.14, y' is not a best approximant of y . \square

To prove the theorem, let us consider a right companion y as in (53). The arguments for a left companion are completely analogous.

First, Lemma 4.15 implies that the best approximants of y are among the rational ideal boundary points of the domains R_x and L'_x (see Figure 17).

Let us first consider the rational ideal boundary points of R_x , which are

$$\gamma_\ell^+(x) = [T]^\ell \cdot \infty \quad \text{for } \ell \in \mathbb{Z}$$

(see Section 4.5). Of these, $y = \gamma_k^+(x)$ and $\infty = \gamma_0^+(x)$ are by definition not best approximants of y .

Next, we will use Lemma 4.14 to show that $\gamma_\ell^+(x)$ is not a best approximant if $k < \ell$ or $\ell < 0$. To see this, note first that the ideal endpoints of the geodesic $[T]^m \cdot g_y$ are

$$\gamma_m^+(x) \quad \text{and} \quad \gamma_{m+k}^+(x).$$

Hence, if

$$k \leq m < \ell < m+k$$

or

$$m < \ell < m+k \leq 0$$

then $[T]^m \cdot g_y$ separates g_y and $\gamma_\ell^+(x)$. Thus we have eliminated all rational ideal boundary points of R_x as best approximants except

$$x = \gamma_1^+(x), \quad \gamma_2^+(x), \quad \dots \quad \gamma_{k-1}^+(x). \quad (54)$$

To eliminate all rational ideal boundary points of L'_x , let $\iota \in \widehat{G}$ be the lift of the elliptic involution on M that maps the geodesic ϱ_x to itself, only reversing its orientation. Then the rational ideal boundary points of L'_x are the numbers

$$\iota \cdot \gamma_\ell^+(x) = \iota \circ [T]^\ell \cdot \infty \quad \text{for } \ell \in \mathbb{Z}$$

Thus, if

$$m < \ell < m+k$$

then the geodesic $\iota \circ [T]^m \circ g_y$ separates g_y and $\iota \circ \gamma_\ell^+(x)$. By Lemma 4.14, this excludes all rational ideal boundary points of L'_x as best companions of y .

Now the only candidates for best approximant of y are the numbers (54), and we know that x and $\gamma_{k-1}^+(x)$ have the same approximation quality. To prove that they are indeed the best approximants, it remains to show (52) for

$$\frac{a}{b} = \gamma_\ell^+(x) \quad \text{with} \quad 1 < \ell < k-1.$$

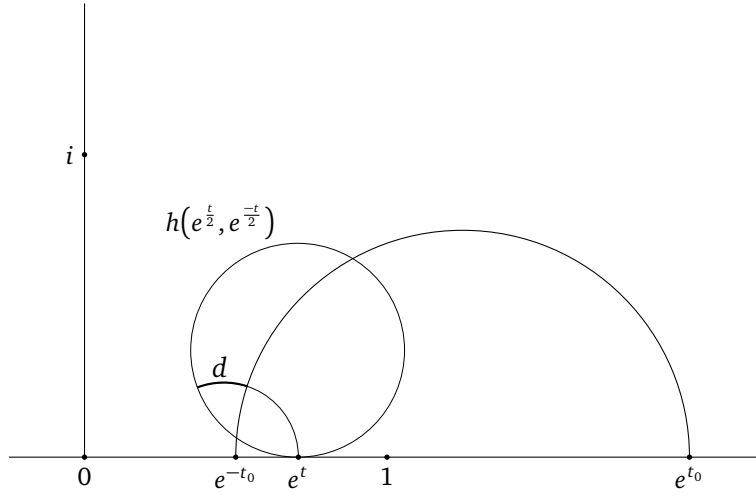


Figure 18: The signed distance d between the geodesic with ideal endpoints $e^{\pm t_0}$ and the horocycle $h(e^{\frac{t}{2}}, e^{-\frac{t}{2}})$

If $k = 2$, there is nothing to show. For $k > 2$, we will take the geometric point of view to simplify the calculations.

We have to show that among the Ford circles at the the rational numbers (54), the minimal signed distance to the vertical geodesic g_y is attained precisely for the first and the last (see Lemma 2.8). Note that the Ford circles at $\gamma_\ell^+(x)$ with $\ell \in \mathbb{Z}$ are equally spaced translates along the translation axis ϱ_x . In particular, all these horocycles have the same signed distance to ϱ_x . Moreover, $1 \leq \ell \leq k - 1$ if and only if g_y separates ϱ_x and the center $\gamma_\ell^+(x)$.

To simplify the calculations, we apply a hyperbolic isometry that maps the axis ϱ_x to the upward oriented vertical geodesic g_0 , and the geodesic g_y to the geodesic with ideal endpoints e^{-t_0} and e^{t_0} for some positive real t_0 (see Figure 18). Then the images of the Ford circles at $\gamma_\ell^+(x)$ are among the 1-parameter family of translates of some horocycle $h(a, a)$ along the axis g_0 . To simplify the calculations further, we will consider the translates of $h(1, 1)$ instead. This scales the horocycles evenly, so all distances change by the same additive constant. That is, we consider the family of horocycles $h(p(t), q(t))$ with

$$\begin{pmatrix} p(t) \\ q(t) \end{pmatrix} = \begin{pmatrix} e^{\frac{t}{2}} & 0 \\ 0 & e^{-\frac{t}{2}} \end{pmatrix} \begin{pmatrix} 1 \\ 1 \end{pmatrix} = \begin{pmatrix} e^{\frac{t}{2}} \\ e^{-\frac{t}{2}} \end{pmatrix}$$

(see Section 2.9 and [13, p. 665], [32, Ch. 5]). Among these, the scaled images of the Ford circles at $\gamma_\ell^+(x)$ are the horocycles $h(e^{\frac{t}{2}}, e^{-\frac{t}{2}})$ with

$$t = \frac{t_0}{k} (2\ell - k). \quad (55)$$

(To see this, note that for integer values of ℓ between 0 and k , the t -values are evenly spaced reals between $-t_0$ and t_0 .)

The signed distance between the horocycle $h(e^{\frac{t}{2}}, e^{-\frac{t}{2}})$ and the geodesic with ideal endpoints $e^{\pm t_0}$ is

$$d = \log \left| f\left(e^{\frac{t}{2}}, e^{-\frac{t}{2}}\right) \right|,$$

where f is a quadratic form on \mathbb{R}^2 with determinant -1 that is zero for $\frac{p}{q} = e^{\pm t_0}$ (see [32, Ch. 10]). This determines f up to sign and we may choose

$$f(p, q) = \frac{1}{\sinh t_0} (p^2 - 2(\cosh t_0) p q + q^2).$$

For $t \in (-t_0, t_0)$ we obtain

$$e^d = \frac{2}{\sinh t_0} (\cosh t_0 - \cosh t). \quad (56)$$

This is a concave even function of t with limit zero as $t \rightarrow \pm t_0$. Hence, for t as in (55) with $\ell \in \mathbb{Z}$ and $1 \leq \ell \leq k-1$, the signed distance d attains its minimum precisely for $\ell = 1$ and $\ell = k-1$. This completes the proof of Theorem 3.15.

4.8 Empty intervals around Markov fractions

This section is about the largest intervals I_x around each Markov fraction x that contain no other Markov fractions (see Section 2.7). At the same time, I_x is the smallest closed interval that contains all companions of x . We will prove Lemmas 4.16 and 4.18, which will be used in the following section to complete the proof of the classification Theorem 2.1.

From the geometric point of view, Lemmas 4.16 and 4.18 are well known, and even in greater generality: for arbitrary hyperbolic tori with one cusp. This is the origin of McShane's remarkable identity for the lengths of simple closed geodesics [21] (see also Remark 4.19), which has been reproved [5, 15, 29] and generalized [2, 22, 23] in various ways. Nevertheless, it seems worthwhile to provide independent proofs in the current context.

Lemma 4.16. *For every Markov fraction $x = \frac{p}{q}$, the interval I_x defined by equation (9) is the smallest closed interval that contains all companions of x . It contains no Markov fractions other than x , nor any of their companions. But the irrational endpoints of I_x are accumulation points of the set of Markov fractions.*

Proof of Lemma 4.16. By equations (41) and (42), the right endpoint ξ_+ of I_x is the limit of the increasing sequence $(\gamma_k^+(x))_{k \geq 2}$ of right companions of x . Analogously or by symmetry, the left endpoint is the limit of the decreasing sequence of left companions. Thus no smaller closed interval contains all companions.

The rational ideal boundary points of the domain L'_x are Markov numbers, and they accumulate at the right endpoint of I_x (see Section 4.6 and Figures 16 and 17). Similarly, the rational ideal boundary points of R'_x are Markov numbers accumulating at the left endpoint of I_x . As accumulations points of Markov

numbers, the endpoints of I_x are irrational (see Section 2.3; in fact, it is well known that the endpoints are Markov irrationals).

For every interior point y of I_x except x , the geodesic $\pi(g_y)$ in M has self-intersections. To see this if $y > x$, note that g_y intersects $[T] \cdot g_y$ (see Section 4.5). The same holds for $y < x$ by an analogous argument or by symmetry. Since the endpoints of I_x are not even rational, this implies that x is the only Markov fraction in I_x .

In particular, this means that no other Markov fraction is between x and one of its companions. Since this is true for all Markov fractions, and they accumulate at the endpoints of I_x , this implies that I_x does not contain any companions of other Markov fractions than x . \square

Corollary 4.17. *For different Markov fractions $x \neq x'$, the interiors \mathring{I}_x and $\mathring{I}_{x'}$ are disjoint.*

Lemma 4.18. *As x ranges over the set of Markov fractions, the intervals I_x cover the set \mathbb{Q} of rational numbers.*

Proof. Since the intervals obviously cover the set of Markov fractions, let us assume that $y \in \mathbb{Q}$ is not a Markov fraction. We have to find a Markov fraction x for which $y \in I_x$.

To this end, define the infinite sequence of centered Markov triples

$$m_k = \left(\frac{p_{k,1}}{q_{k,1}}, \frac{p_{k,2}}{q_{k,2}}, \frac{p_{k,3}}{q_{k,3}} \right)$$

with

$$\frac{p_{k,1}}{q_{k,1}} < y < \frac{p_{k,3}}{q_{k,3}} \quad (57)$$

recursively by

- $m_0 = (\lfloor y \rfloor, \lfloor y \rfloor + \frac{1}{2}, \lfloor y \rfloor + 1)$, where $\lfloor y \rfloor$ denotes the largest integer not larger than y , and
- for $k > 0$, the triple m_k is the child satisfying (57) among the two children of m_{k-1} in the tree of centered rational Markov triples (see Lemma 3.8).

First consider the following two cases:

1. The triple m_k is the left child of m_{k-1} for all but finitely many k .

That is, the sequence of Markov fractions $\frac{p_{k,1}}{q_{k,1}}$ eventually becomes constant, say

$$\frac{p_{k,1}}{q_{k,1}} = x \quad \text{for } k > k_0,$$

while $\frac{p_{k,2}}{q_{k,2}}$ and $\frac{p_{k,3}}{q_{k,3}}$ are consecutive ideal boundary points of L'_x with

$$\lim \frac{p_{k,2}}{q_{k,2}} = \lim \frac{p_{k,3}}{q_{k,3}} = \xi_+$$

(see Section 4.6 and Figures 16 and 17). Hence $y \in I_x$

2. The triple m_k is the right child of m_{k-1} for all but finitely many k .

In this case,

$$\frac{p_{k,3}}{q_{k,3}} = x \quad \text{for } k > k_0,$$

and like in case 1 we see that $y \in I_x$.

We will complete the proof of the lemma by showing that the third case does not occur:

3. Infinitely many of the triples m_k are left children of m_{k-1} and infinitely many are right children.

For such a sequence of rational Markov triples, we will show that

$$\lim \left(\frac{p_{k,3}}{q_{k,3}} - \frac{p_{k,1}}{q_{k,1}} \right) = 0. \quad (58)$$

Then condition (57) would imply

$$\lim \frac{p_{k,1}}{q_{k,1}} = y = \lim \frac{p_{k,3}}{q_{k,3}}.$$

This would contradict y being rational, because accumulation points of the set of Markov fractions are irrational (see Section 2.3).

It remains to show (58) in case 3. To this end, note that for any rational Markov triple $(\frac{p_1}{q_1}, \frac{p_2}{q_2}, \frac{p_3}{q_3})$ we have

$$\begin{aligned} \frac{p_3}{q_3} - \frac{p_1}{q_1} &= \left(\frac{p_3}{q_3} - \frac{p_2}{q_2} \right) + \left(\frac{p_2}{q_2} - \frac{p_1}{q_1} \right) \\ &\stackrel{(16)}{=} \frac{q_1}{q_2 q_3} + \frac{q_3}{q_1 q_2} \\ &\stackrel{(17)}{=} \frac{q_1 + q_3}{q_1 q_2} \\ &\stackrel{(14)}{=} 3 - \frac{q_2}{q_3 q_1}, \end{aligned}$$

so it is enough to show

$$\lim \frac{q_{k,2}}{q_{k,3} q_{k,1}} = 3. \quad (59)$$

To see this, we will show that for any centered rational Markov triple $(\frac{p_1}{q_1}, \frac{p_2}{q_2}, \frac{p_3}{q_3})$ we have

$$\frac{q_2}{q_3 q_1} \geq \frac{3}{1 + \frac{1}{q_1} + \frac{1}{q_3}}. \quad (60)$$

Since both sequences $(q_{k,1})$ and $(q_{k,3})$ are unbounded in case 3, equation (59) follows.

Finally, to prove the estimate (60) for a centered rational Markov triple, note that (24) implies

$$\frac{q_2}{q_3 q_1} \geq \max \left\{ \frac{q_1}{q_2 q_3}, \frac{q_3}{q_1 q_2} \right\},$$

and with equation (14),

$$\frac{q_2}{q_3 q_1} \geq 1,$$

Hence $\frac{q_2}{q_1} \geq q_3$ and therefore

$$\frac{q_1}{q_2 q_3} = \frac{q_2}{q_3 q_1} \cdot \frac{q_1^2}{q_2^2} \leq \frac{q_2}{q_3 q_1} \cdot \frac{1}{q_3^2}.$$

In the same way we get $\frac{q_2}{q_3} \geq q_1$ and

$$\frac{q_3}{q_1 q_2} \leq \frac{q_2}{q_3 q_1} \cdot \frac{1}{q_1^2}.$$

Now equation (14) yields

$$3 \leq \frac{q_2}{q_3 q_1} \left(\frac{1}{q_3^2} + 1 + \frac{1}{q_1^2} \right)$$

and hence (60). This completes the proof of Lemma 4.18. \square

Remark 4.19. McShane's identity [21] says that

$$\sum_{\gamma} \frac{1}{1 + e^{|\gamma|}} = \frac{1}{2}, \quad (61)$$

where the sum is taken over all simple closed geodesics in some hyperbolic torus with one cusp, and $|\gamma|$ denotes the length of the geodesic. For the modular torus M , this identity can be derived as follows. The unoriented closed geodesics in M are in one-to-one correspondence with the $(\text{mod } 3)$ -equivalence classes of Markov fractions. The length of the closed geodesic η_x and the length of the interval I_x are related by

$$\frac{1}{1 + e^{|\gamma|}} = \frac{1}{6} |I_x| \quad (62)$$

(see Remark 4.6). On the other hand, Corollary 4.17 and Lemma 4.18 imply

$$2 \sum_x |I_x| = 6 \quad (63)$$

which yields McShane's identity.

4.9 Proof of Theorem 2.1 (Classification)

Since we have already proved Theorems 3.6 and 3.15 in the two previous sections, we only have to show that $C(y) < \frac{1}{3}$ if y is a rational number y that is neither a Markov fraction nor a companion of a Markov fraction.

By Lemma 4.18 there is a Markov fraction x such that $y \in I_x$. Since we assume that y is not a Markov fraction or a companion, Lemma 4.16 implies that y lies between two companions of x or between x and one of its first companions. In other words, there is an integer $k \geq 1$ such that

$$\gamma_{k+1}^-(x) < y < \gamma_k^-(x) \quad \text{or} \quad \gamma_k^+(x) < y < \gamma_{k+1}^+(x).$$

We will show that there is not enough space between the Ford circles at $\gamma_k^\pm(x)$ and $\gamma_{k+1}^\pm(x)$ such that a vertical geodesic could pass between them and stay at least a signed distance of $\log \frac{2}{3}$ away from both. With Corollary 2.9, this shows that $C(y) < \frac{1}{3}$.

We already know that

$$\left| \gamma_k^\pm(x) - \gamma_{k+1}^\pm(x) \right| = \frac{1}{qu_k u_{k+1}}, \quad (64)$$

and since the denominator a companion $\gamma_k^\pm(x)$ is qu_k , the euclidean radius of its Ford circle is

$$\frac{1}{2q^2 u_k^2}$$

(see equation (51), Lemma 3.10, and Section 2.9). A necessary condition for $C(y) \geq \frac{1}{3}$ is that the vertical geodesic g_y fits between the Ford circles at $\gamma_k^\pm(x)$ and $\gamma_{k+1}^\pm(x)$, scaled by $\frac{2}{3}$ in the euclidean metric (see Corollary 2.9 and Figure 1). Therefore, to prove that $C(y) < \frac{1}{3}$, it suffices to show that

$$\left| \gamma_{k+1}^\pm(x) - \gamma_k^\pm(x) \right| < \frac{1}{3q^2 u_{k+1}^2} + \frac{1}{3q^2 u_k^2}. \quad (65)$$

And indeed we have

$$\begin{aligned} \frac{1}{3q^2 u_{k+1}^2} + \frac{1}{3q^2 u_k^2} &= \frac{u_k^2 + u_{k+1}^2}{3q^2 u_k^2 u_{k+1}^2} \\ &\stackrel{(36)}{=} \frac{3qu_k u_{k+1} + 1}{3q^2 u_k^2 u_{k+1}^2} \\ &= \frac{1}{qu_k u_{k+1}} + \frac{1}{3q^2 u_k^2 u_{k+1}^2} \\ &\stackrel{(64)}{>} \left| \gamma_k^\pm(x) - \gamma_{k+1}^\pm(x) \right|. \quad \square \end{aligned}$$

4.10 Proof of Theorems 2.5 and 2.7 (Triangle paths)

The Epstein–Penner convex hull construction [12] provides the modular torus M with a euclidean metric, with respect to which the ideal hyperbolic triangles of the canonical triangulation are equilateral euclidean triangles. We may assume that the developing map $D : H^2 \rightarrow \mathbb{C}$ maps the ideal triangle $\infty, 0, 1$ to the euclidean triangle $0, 1, \omega$ with ω as in Theorem 2.5. The image of D is then the complement $\mathbb{C} \setminus \Gamma$ of the Eisenstein lattice $\Gamma = \mathbb{Z} + \omega\mathbb{Z}$. The canonical projection π factors through $\mathbb{C} \setminus \Gamma$, giving rise to the projection $\bar{\pi}$:

$$\begin{array}{ccc} H^2 & \xrightarrow{D} & \mathbb{C} \setminus \Gamma \\ \downarrow \pi & \swarrow \bar{\pi} & \\ M & & \end{array}$$

If m and n are coprime integers, then the projection $\bar{\pi}$ maps the oriented line segment from 0 to $z_{m,n} = m + n\omega$ to a simple closed curve in M . There is a unique homotopic simple geodesic in M with both ends in the cusp (under homotopy with ends in the cusp), and all simple geodesics with both ends in the cusp can be obtained in this way. If m and n are both nonnegative, the geodesic in M lifts to a vertical geodesic g_x in H^2 , oriented from ∞ to 0 , where x is a Markov fraction between 0 and 1 . As the geodesic g_x traverses finitely many triangles of the Farey triangulation, the new vertices are obtained by Farey addition. But the developing map D maps the triangles of the Farey triangulation that g_y traverses to the regular euclidean triangles that the line segment from 0 to $z_{m,n}$ traverses. Hence, the Markov fraction x can also be obtained by Farey addition along the euclidean triangle strip. This proves Theorem 2.5.

To prove Theorem 2.7 in a similar fashion, note that $\bar{\pi}$ projects the deformed straight line segments to curves in M with both ends in the cusp that cross neither the respective simple geodesic with both ends in the cusp nor the corresponding simple closed geodesic.

Acknowledgement. I would like to thank Gergely Harcos, who graciously made me aware of the previous results by Flahive [14] and Gurwood [17].

This research was supported by DFG SFB/TR 109 “Discretization in Geometry and Dynamics”.

References

- [1] M. Aigner. *Markov’s theorem and 100 years of the uniqueness conjecture*. Springer, Cham, 2013.
- [2] H. Akiyoshi, H. Miyachi, and M. Sakuma. A refinement of McShane’s identity for quasifuchsian punctured torus groups. In *In the tradition of Ahlfors and*

- Bers, III*, volume 355 of *Contemp. Math.*, pages 21–40. Amer. Math. Soc., Providence, RI, 2004.
- [3] A. I. Bobenko, U. Pinkall, and B. A. Springborn. Discrete conformal maps and ideal hyperbolic polyhedra. *Geom. Topol.*, 19(4):2155–2215, 2015.
 - [4] F. Bonahon. *Low-dimensional geometry*, volume 49 of *Student Mathematical Library*. Amer. Math. Soc., Providence, RI, 2009.
 - [5] B. H. Bowditch. A proof of McShane’s identity via Markoff triples. *Bull. London Math. Soc.*, 28(1):73–78, 1996.
 - [6] J. W. S. Cassels. *An introduction to Diophantine approximation*. Cambridge University Press, New York, 1957.
 - [7] H. Cohn. Approach to Markoff’s minimal forms through modular functions. *Ann. of Math. (2)*, 61:1–12, 1955.
 - [8] H. Cohn. Representation of Markoff’s binary quadratic forms by geodesics on a perforated torus. *Acta Arith.*, 18:125–136, 1971.
 - [9] J. H. Conway. *The sensual (quadratic) form*, volume 26 of *Carus Mathematical Monographs*. Mathematical Association of America, Washington, DC, 1997.
 - [10] T. W. Cusick and M. E. Flahive. *The Markoff and Lagrange spectra*. Amer. Math. Soc., Providence, RI, 1989.
 - [11] M. Einsiedler and T. Ward. *Ergodic theory with a view towards number theory*, volume 259 of *Graduate Texts in Mathematics*. Springer-Verlag London, Ltd., London, 2011.
 - [12] D. B. A. Epstein and R. C. Penner. Euclidean decompositions of noncompact hyperbolic manifolds. *J. Differential Geom.*, 27(1):67–80, 1988.
 - [13] V. V. Fock and A. B. Goncharov. Dual Teichmüller and lamination spaces. In A. Papadopoulos, editor, *Handbook of Teichmüller theory. Vol. I*, pages 647–684. Eur. Math. Soc., Zürich, 2007.
 - [14] M. E. [Flahive] Gbur. On the minimum of zero indefinite binary quadratic forms. *Mathematika*, 25(1):94–106, 1978.
 - [15] C. Goodman-Strauss and Y. Rieck. Simple geodesics on a punctured surface. *Topology Appl.*, 154(1):155–165, 2007.
 - [16] D. S. Gorshkov. Geometry of Lobachevskii in connection with certain questions of arithmetic (Russian). *Zap. Nauchn. Semin. Leningr. Otd. Mat. Inst. Steklova*, 76:39–85, 1977. English translation in *J. Soviet Math.* 16 (1981) 788–820.
 - [17] C. Gurwood. *Diophantine approximation and the Markov chain*. PhD thesis, New York University, 1976.
 - [18] A. Haas. Diophantine approximation on hyperbolic Riemann surfaces. *Acta Math.*, 156(1-2):33–82, 1986.
 - [19] G. H. Hardy and E. M. Wright. *An introduction to the theory of numbers*. Oxford University Press, Oxford, sixth edition, 2008.

- [20] A. Hatcher. Topology of numbers. Book preprint, <https://www.math.cornell.edu/~hatcher/TN/TNpage.html> (accessed 2022-09-21).
- [21] G. McShane. *A remarkable identity for lengths of curves*. PhD thesis, University of Warwick, 1991. <http://wrap.warwick.ac.uk/4008/>.
- [22] G. McShane. Simple geodesics and a series constant over Teichmüller space. *Invent. Math.*, 132(3):607–632, 1998.
- [23] G. McShane. Weierstrass points and simple geodesics. *Bull. London Math. Soc.*, 36(2):181–187, 2004.
- [24] G. McShane and H. Parlier. Multiplicities of simple closed geodesics and hypersurfaces in Teichmüller space. *Geom. Topol.*, 12(4):1883–1919, 2008.
- [25] R. C. Penner. The decorated Teichmüller space of punctured surfaces. *Comm. Math. Phys.*, 113(2):299–339, 1987.
- [26] R. C. Penner. *Decorated Teichmüller theory*. QGM Master Class Series. European Mathematical Society (EMS), Zürich, 2012.
- [27] J. Propp. The combinatorics of frieze patterns and Markoff numbers. *Integers*, 20, 2020.
- [28] A. M. Rockett and P. Szűsz. *Continued fractions*. World Scientific Publishing Co., Inc., River Edge, NJ, 1992.
- [29] T. A. Schmidt and M. Sheingorn. McShane’s identity, using elliptic elements. *Geom. Dedicata*, 134:75–90, 2008.
- [30] P. Schmutz. Systoles of arithmetic surfaces and the Markoff spectrum. *Math. Ann.*, 305(1):191–203, 1996.
- [31] C. Series. The geometry of Markoff numbers. *Math. Intelligencer*, 7(3):20–29, 1985.
- [32] B. Springborn. The hyperbolic geometry of Markov’s theorem on Diophantine approximation and quadratic forms. *Enseign. Math.*, 63(3-4):333–373, 2017.
- [33] D. Zagier. On the number of Markoff numbers below a given bound. *Math. Comp.*, 39(160):709–723, 1982.

Boris Springborn <boris.springborn@tu-berlin.de>

Technische Universität Berlin
 Institut für Mathematik, MA 8-3
 Str. des 17. Juni 136
 10623 Berlin, Germany